Working Document

Post-cruise meeting of the Working Group on International Pelagic Surveys (WGIPS)
Copenhagen, Denmark, 19 – 21 June 2018

Working Group on Widely distributed Stocks
Tórshavn, Faroe Islands, 28 August - 3 September 2018

INTERNATIONAL ECOSYSTEM SURVEY IN NORDIC SEA (IESNS) in May – June 2018

Maxim Rybakov[4], Tatyana Sergeeva[4], Anna Gordeeva[4]
RV Vilnyus

Valantine Anthonypillai[2], Are Salthaug[2], Erling Kåre Stenevik[2], Kjell Arne Mork[2], Cecilie Thorsen Broms[2], Øystein Skagseth[2]
RV G.O. Sars

Karl-Johan Stæhr[3], Benoît Bergès[6], Mathias Kloppmann[8], Sven Kupschus[9]
RV Dana

Guðmundur J. Óskarsson[7], Anna Heiða Ólafsdóttir[7], Hildur Pétursdóttir[7]
RV Árni Friðriksson

Eydna í Homrum[5], Ebba Mortensen[5], Sólva Eliassen[5], Poul Vestergaard[5], Leon Smith[5]
RV Magnus Heinason

2 Institute of Marine Research, Bergen, Norway
3 DTU-Aqua, Denmark
4 PINRO, Murmansk, Russia
5 Faroese Marine Research Institute, Tórshavn, Faroe Islands
6 Wageningen Marine Research, IJmuiden, The Netherlands
7 Marine and Freshwater Research Institute, Reykjavik, Iceland
8 vTI-SF, Hamburg, Germany
9 Cefas, Lowestoft, UK

Introduction

In May-June 2018, five research vessels; R/V Dana, Denmark (joined survey by Denmark, Germany, Ireland, The Netherland, Sweden and UK), R/V Magnus Heinason, Faroe Islands, R/V Árni Friðriksson, Iceland, R/V G.O. Sars Norway and R/V Vilnyus, Russia participated in the International ecosystem survey in the Nordic Seas (IESNS). The aim of the survey was to cover the whole distribution area of the Norwegian Spring-spawning herring with the objective of estimating the total biomass of the herring stock, in addition to collect data on plankton and hydrographical conditions in the area. The survey was initiated by the Faroes, Iceland, Norway and Russia in 1995. Since 1997 also the EU participated (except 2002 and 2003) and from 2004 onwards it was more integrated into an ecosystem survey. This report is compilation of data from this International survey stored in the PGNAPES database and supported by national survey reports from each survey (Dana: Staehr, Bergès, Kloppmann, Kupschus 2018, Magnus Heinason: Homrum, Eliasen, FAMRI 1820-2018, Árni Friðriksson: Óskarsson et al. 2018, Vilnyus: Rybakov PINRO 2018).

Material and methods

Coordination of the survey was done during the WGIPS meeting in January 2018. The participating vessels together with their effective survey periods are listed in the table below:

Vessel	Institute	Survey period
Dana	Danish Institute for Fisheries Research, Denmark	1/5-30/05
G.O. Sars	Institute of Marine Research, Bergen, Norway	30/4-2/6
Vilnyus	PINRO, Russia	23/5–16/6
Magnus Heinason	Faroe Marine Research Institute, Faroe Islands	03/5- 15/5
Árni Friðriksson	Marine and Freshwater Research Institute, Iceland	05/5-19/5

Figure 1 shows the cruise tracks and the CTD/WP-2 stations and Figure 2 the cruise tracks and the trawl stations. Survey effort by each vessel is detailed in Table 1. Frequent contacts were maintained between the vessels during the course of the survey, primarily through electronic mail. The temporal progression of the survey is shown in Figure 4.

In general, the weather condition did not affect the survey even if there were some days that were not favorable and prevented for example WP2 and MOCNESS sampling at some stations. The survey was based on scientific echosounders using 38 kHz frequency. Transducers were calibrated with the standard sphere calibration (Foote *et al*., 1987) prior to the survey. Salient acoustic settings are summarized in the text table below.

Acoustic instruments and settings for the primary frequency (boldface).

	Dana	G.O. Sars	Arni Friðriksson	Magnus Heinason	Vilnyus
Echo sounder	Simrad EK 60	Simrad EK 80	Simrad EK60	Simrad EK60	Simrad EK60
Frequency (kHz)	**38**	**38**, 18, 70, 120, 200, 333	**38**, 18, 120, 200	**38**,200	**38,** 120
Primary transducer	ES38BP	ES 38B	ES38B	ES38B	ES38B
Transducer installation	Towed body	Drop keel	Drop keel	Hull	Hull
Transducer depth (m)	5	8.5	8	3	4.5
Upper integration limit (m)	5	15	15	7	10
Absorption coeff. (dB/km)	10	9.8	10	10.1	10
Pulse length (ms)	1.024	1.024	1.024	1.024	1.024
Band width (kHz)	1.573	2.43	2.425	2425	2.425
Transmitter power (W)	2000	2000	2000	2000	2000
Angle sensitivity (dB)	21.9	21.9	21.9	21.9	21.9
2-way beam angle (dB)	-20.5	-20.7	-20.81	-20.8	-20.6
Sv Transducer gain (dB)					
Ts Transducer gain (dB)	25.32	26.25	24.34	25.67	25.76
s_A correction (dB)	-0.56	-0.13	-0.61	-0.73	-0.64
3 dB beam width (dg)					
alongship:	6.8	6.4	7.28	7.15	7.09
athw. ship:	6.8	6.35	7.23	7.08	7.01
Maximum range (m)	500	500	500	500	500
Post processing software	LSSS	LSSS	LSSS	Sonardata Echoview 8.1	LSSS

Post-processing software differed among the vessels but all participants used the same post-processing procedure, which is according to an agreement at a PGNAPES scrutinizing workshop in Bergen in February 2009 (ICES 2009), and "Notes from acoustic Scrutinizing workshop in relation to the IESNS", Reykjavík 3.-5. March 2015 (Annex 4 in ICES 2015).
Generally, acoustic recordings were scrutinized on daily basis and species identified and partitioned using catch information, characteristic of the recordings, and frequency between integration on 38 kHz and on other frequencies by a scientist experienced in viewing echograms. All vessels used a large or medium-sized pelagic trawl as the main tool for biological sampling. The salient properties of the trawls are as follows:

	Dana	G.O. Sars	Arni Friðriksson	Magnus Heinason	Vilnyus
Circumference (m)		832	832	640	500
Vertical opening (m)	25-35	30–50	30–35	45–55	50
Mesh size in codend (mm)		40	40	40	16
Typical towing speed (kn)	3.5-4.0	3.0–4.5	3.1–5.0	3.0–4.0	3.3–4.5

Catches from trawl hauls were sorted and weighed; fish were identified to species level, when possible, and other taxa to higher taxonomic levels. Normally, a subsample of 30–100 herring, blue whiting and mackerel were sexed, aged, and measured for length and weight, and their maturity status was estimated using established methods. For the Norwegian, Icelandic and Faroese vessel, a smaller subsample of stomachs was sampled for further analyses on land. An additional sample of 70–300 fish was measured for length.

Acoustic data were analysed using the StoX software package recently adopted for WGIPS coordinated surveys. A description of StoX can be found here: http://www.imr.no/forskning/prosjekter/stox/nb-no. Estimation of abundance from acoustic surveys with StoX is carried out according to the stratified transect design model developed by Jolly and Hampton (1990). This method requires pre-defined strata, and the survey area was therefore split into 5 strata with pre-defined acoustic transects as agreed during the WGIPS in January 2017. Within each stratum, parallel transects with equal distances were used. The distance between transects was based on available survey time, and the starting point of the first transect in each stratum was randomized. This approach allows for robust statistical analyses of uncertainty of the acoustic estimates. The strata and transects used in StoX are shown in Figure 3. All trawl stations within a given stratum with catches of the target species (either blue whiting or herring) were assigned to all transects within the stratum, and the length distributions were weighted equally within the stratum. The following target strength (TS)-to-fish length (L) relationships were used:

Blue whiting: $TS = 20 \log(L) - 65.2$ dB (ICES 2012)

Herring: $TS = 20.0 \log(L) - 71.9$ dB

The target strength for herring is the traditionally one used while this target strength for blue whiting was first applied in 2012 (ICES 2012).

In StoX a superindividual table is produced where abundance is linked to population parameters like age, length, weight, sex, maturity etc. (exact name: 1_FillMissingData_SuperIndividuals.txt). This table can be used to split the total abundance estimate by any combination of population parameters.

The hydrographical and plankton stations by survey are shown in Figure 1. Most vessels collected hydrographical data using a SBE 911 CTD. Maximum sampling depth was 1000 m. Zooplankton was sampled by a WPII on all vessels except the Russian vessel which used a Djedi net, according to the standard procedure for the surveys. Mesh sizes were 180 or 200 µm. The net

was hauled vertically from 200 m to the surface or from the bottom whenever bottom depth was less than 200 m. All samples were split in two and one half was preserved in formalin while the other half was dried and weighed. On the Danish, the Icelandic, the Faroese and the Norwegian vessels the samples for dry weight were size fractionated before drying. Data are presented as g dry weight per m^2. For the zooplankton distribution map, all stations are presented. For the time series, stations in the Norwegian Sea delimited to east of 14°W and west of 20°E have been included. The zooplankton data were interpolated using objective analysis utilizing a Gaussian correlation function to obtain a time-series for four different areas. The results are given as inter-annual indexes of zooplankton abundance in May. This method was introduced at WGINOR in 2015 (ICES, 2016) and the results match the former used average index. It has been noted that the Djedy net applied by the Russian vessel in the Barents Sea seems to be less effective in catching zooplankton in comparison to WP2 net applied by other vessels in an overlapping area. Thus, the biomass estimates for the Barents Sea are not directly comparable to the other areas, but are comparable among years within the Barents Sea.

Some preliminary results from ongoing work with sonar and the deep vision system are presented as appendices to this report (Appendix 2-4), but they were not discussed at the post-cruise meeting. In addition, corrected IESNS estimates for 2017 (blue whiting and herring in the Norwegian Sea; ICES 2018) are shown in Appendix 1.

Results and Discussion

Hydrography

The temperature for selected depths in the Norwegian Sea is shown in Figure 5. The temperature distributions in the ocean, averaged over selected depth intervals; 0-50 m, 50-200 m, and 200-500 m, are then shown in Figures 6-8. The temperatures in the surface layer (0-50 m) ranged from 0°C in the Iceland and Greenland Sea to 9°C in the southern part of the Norwegian Sea (Fig. 6). The Iceland-Faroe Front was encountered slightly south of 65°N east of Iceland extending eastwards towards about 0° west where it turned almost straight northwards. This front was well-defined at 200-500 m depth while shallower it was more diffuse. Further to west at about 8°W, the Jan Mayen Front runs northwards towards Jan Mayen, this front was distinct throughout the observed water column. The warmer North Atlantic water formed a broad tongue that stretched far northwards along the Norwegian coast with temperatures > 7 °C to 70° N in the surface layer.

Relative to a 23 years long-term mean, from 1995 to 2017, the temperatures at 0-50 m and 50-200 m over the western and central Norwegian Sea, roughly west of the 0 meridian, were higher in 2018 compared to the long-term mean (Figures 6 and 7). Relative warmest water was in the western Norwegian Sea where the temperatures in some regions were 1.5 °C higher than the mean. In the eastern area of the Norwegian Sea, along the continental shelf, the temperatures were instead lower than normal, particular in the south where temperatures in some areas were 0.5 °C lower than the mean. At 200-500 m depth no clear regional deviances from the long-term means could be observed (Figure 8). It should also be noted that the temperature in the southwestern region, i.e. south of the Iceland-Faroe Ridge, were lower that the long-term mean.

The temperature, salinity and potential density in the upper 800 m at the Svinøy section in May 2018 is shown in Figure 9. Atlantic water is lying over the colder and fresher intermediate layer and reach down to 500 m at the shelf edge and shallower westward. The warmest water is located near the shelf edge where the core of the inflowing Atlantic Water is located. Westward temperature and salinity are reduced due to mixing with colder and less saline water. Relative to a long-term mean, from 1978 to 2007, the temperatures were higher in 2018 on the shelf and at the shelf edge where the main northward transport of Atlantic Water is located. Further west the temperatures in the upper layer were in general lower than long-term mean.

The Norwegian Atlantic Current (NWAC) and the East Icelandic Current are the two main features of the circulation in the Norwegian Sea where the herring stock is grazing. The NWAC with its offshoots forms the northern limb of the North Atlantic current system and carries relatively warm and salty water from the North Atlantic into the Nordic Seas. The EIC, on the other hand, carries Arctic waters. To a large extent this water derives from the East

Greenland Current, but to a varying extent, some of its waters may also have been formed in the Iceland and Greenland Seas. The EIC flows into the southwestern Norwegian Sea where its waters subduct under the Atlantic waters to form an intermediate Arctic layer. While such a layer has long been known in the area north of the Faroes and in the Faroe-Shetland Channel, it is only in the last three decades that a similar layer has been observed all over the Norwegian Sea.

This circulation pattern creates a water mass structure with warm Atlantic Water in the eastern part of the area and more Arctic conditions in the western part. The NWAC is rather narrow in the southern Norwegian Sea, but when meeting the Vøring Plateau off Mid Norway it is deflected westward. The western branch of the NWAC reaches the area of Jan Mayen at about 71°N. Further northward in the Lofoten Basin the lateral extent of the Atlantic water gradually narrows again, apparently under topographic influence of the mid-ocean ridge. It has been shown that atmospheric forcing largely controls the distribution of the water masses in the Nordic Seas. Hence, the lateral extent of the NWAC, and consequently the position of the Arctic Front, that separates the warm North Atlantic waters from the cold Arctic waters, is correlated with the large-scale distribution of the atmospheric sea level pressure. The local air-sea heat flux in addition influence the upper layer and it is found that it can explain about half of the year to year variability of the ocean heat content in the Norwegian Sea.

Zooplankton

The zooplankton biomass (g dry weight m^{-2}) in the upper 200 m is shown in Figure 10. Sampling stations were evenly spread over the area, and most oceanographic regions were covered. The Svinøy transect is also shown in the figure. The high zooplankton biomasses were spread over several locations covering the entire sampling area, maybe except from the most north-eastern area which contained intermediate biomasses. High biomasses were found southwest of Lofoten, in the southern Norwegian Sea, south in the Lofoten Basin, and in western and north western areas towards the Jan Mayen and Mohn ridge.

Figure 11 shows the zooplankton index given for the sampling area (delimited to east of 14°W and west of 20°E), and for four sub-areas. The zooplankton biomass index for the Norwegian Sea and nearby areas in 2018 was 8.8 g dry weight m^{-2}, which is a small decrease from last year (Figure 11). A similar decrease was observed in all sub-areas, except from East of Iceland.

The zooplankton biomass index for the Norwegian Sea in May has been estimated since 1995. For the period 1995-2002 the plankton index was relatively high (mean 11.2 g) even if varying between years. From 2003-2006, the index decreased continuously and has been at lower levels since then (mean 7.7 g for the period 2003-2018). However, an increase can be noted in the last part of the low-biomass period. This general pattern applies more or less to all the different sub-areas within the Norwegian Sea. The zooplankton biomass east of Iceland was, however, in general higher compared with the other sub-areas until 2015.

The reason for this fluctuation in the zooplankton biomass is not obvious to us. The unusually high biomass of pelagic fish feeding on zooplankton has been suggested to be one of the main causes for the reduction in zooplankton biomass. However, carnivorous zooplankton and not

pelagic fish are the main predators of zooplankton in the Norwegian Sea (Skjoldal *et al.,* 2004), and we do not have good data on the development of the carnivorous zooplankton stocks. Timing effects, as match/mismatch with the phytoplankton bloom, can also affect the zooplankton abundance. Also the time of entry of fish into the area, i.e. the residence of forage fish in the area, in relation to the sampling period might complicate inferences from such data. More ecological and environmental research to reveal inter-annual variations and long-term trends in zooplankton abundance are recommended. Quantitative research on carnivorous zooplankton stocks (such as krill and amphipods) across the whole survey area is an important step in that direction and needs a further effort by all participating countries.

Norwegian spring-spawning herring

Survey coverage in the Norwegian Sea was considered adequate in 2018 and in line with previous years. The zero-line was believed to be reached for adult NSS herring throughout the area. It is therefore recommended that the results can be used for assessment purpose. The herring was primarily distributed in the southwestern Norwegian Sea (Figure 12). In the Barents Sea the main aggregations were observed in the eastern part. Registrations of NSS herring were low in the eastern part of the Norwegian Sea. In the southernmost part of the survey area herring was also observed (Figure 12a), but based on the otolith structure a significant part of this herring was of autumn spawning type.

As in previous years the size and age of herring were found to increase towards west and south in the Norwegian Sea (Figure 13). Correspondingly, it was mainly older herring that appeared in the southwestern areas. The 2013 year class (age 5) was observed across most of the survey area, but in low quantity in the western most areas.

Five year old herring (year class 2013) dominated both in terms of number (29 %) and biomass (25 %) on basis of the StoX estimations for Norwegian Sea (Table 2). Its number at age 5 (Table 2) is two times higher than for the 2009 year class at same age, but only half the size of the large 2004 year class (Figure 14), which puts the size of the 2013 year class into a perspective. Each of three older age groups (age 12-14), which have dominated in the stock in previous years, contributed to ~8 % in number and 10 % in biomass, respectively. Thus, they are still contributing to 30 % of the total biomass. Uncertainty estimates for number at age based on bootstrapping within StoX are shown in Figure 15.

The total estimate of herring in the Norwegian Sea from the 2018 survey was 19.7 billions in number and the biomass 5.04 million tonnes. This estimate is 0.84 million tonnes (20 %) increase from the 2017 survey estimate (Annex 1; corrected estimates). The biomass estimate decreased from 2009 to 2012, and has since then been rather stable at 4.2 to 5.9 million tonnes with similar confidence interval (Figure 16), with the lowest abundance occurring in 2017. The increase in total biomass estimate of herring between 2017 and 2018 is largely driven by the 2013 year class, which constituted to 17 % of the biomass in 2017 while 25 % in 2018. The 2014 year class contributed also to the increase in the biomass estimations between these two years.

The abundance estimates of herring by age and length in the Barents Sea (Stratum 6) are shown in Table 3. The herring at age 2 was in the highest number (17 billions, mean length 17.2 cm and mean weight 33.4 g), but age 1 was also in significant amount (6.8 billions, mean length 10.5 cm and mean weight 7.0 g). The survey estimates of age 1 and 2 from the period 1991-2018 are shown in Figure 17. It indicates that the number of age 2 in 2018 is the fifth highest in the time series. This year class from 2016 was also relatively numerous at age 1 in 2017. However, the uncertainty around these estimates are large, and larger than indicated on Figure 17 as it only accounts for the sampling variability but not for the uncertainty related to spatial restriction and number of biological samples behind the estimates. Moreover, the zero-line of juvenile herring distributions towards north was apparently not reached in Barents Sea as indicated on Figure 12 where herring was registered on the inter-transects.

In the recent four years there have been concerns regarding age reading of herring, because the age distributions from the different participants have showed differences. A scale and otolith exchange has been ongoing for some period, where scales and otoliths for the same fish have been sampled. On basis of that work, a workshop was planned in the spring 2018 to discuss the results. This workshop was postponed until the autumn 2018. The survey group emphasizes the necessity of having this workshop before next year's survey takes place.

With respect to age-reading concerns in the recent years, the comparison between the nations in this year's survey showed a similar difference as observed in recent years (Figure 23). For example, the 2004 year class was in higher proportion by the Norwegian readers than the Faroese and the Icelandic readers in Stratum 3 and 4, which had higher proportion the 2005 and 2006 year classes. These three year classes are combined as plus group in the analytical assessment (age 12+).

In the 2018 IESNS there were no big discrepancies in the acoustic scrutinizing results between any neighboring vessels. An observed difference in acoustic registrations between RV Dana and neighboring vessels west of Jan Mayen (~70°N and 4°E) was related to a bad weather experienced by RV Dana there. In the western part of the survey area, where the highest concentrations of herring were observed, there was a good agreement between any neighboring vessels.

Blue whiting

The spatial distribution of blue whiting in 2018 was similar to the years before, with the highest abundance estimates in the southern and eastern part of the Norwegian Sea, along the Norwegian continental slope. The main concentrations were observed in connections with the continental slopes of Norway and along the Scotland – Iceland ridge (Figure 18). Blue whiting was not distributed as far west into the Norwegian Sea as in the last ~five years and there was less overlap in distribution of herring and blue whiting this year. The largest fish were found in the western and northern part of the survey area (Figure 19). It should be noted that the spatial survey design was not intended to cover the whole blue whiting stock during this period.

The total biomass index of blue whiting registered during the IESNS survey in 2018 was 0.50 million tonnes, which is a 46 % decrease from the biomass estimate in 2017 (0.93). The abundance index for 2018 was 4.4 billion, which is about 54 % lower than in 2017. Ages 2-4 are dominating the biomass (79 % of the biomass and 78% by number). Uncertainty estimates for numbers at age based on bootstrapping with StoX are shown in Figure 20.

In this year's IESNS survey, two year old blue whiting was more numerous as compared to IESNS 2017 and IBWSS 2018 (International Blue Whiting Spawning Survey). The survey group compared age and length distributions by vessel and strata and found some differences in length distributions (Figure 24) by vessel within strata but significant differences in age distribution by vessel within strata (Figure 25) particularly in strata 1 and 2. The survey group could not conclude if the changes in length distribution were enough to explain the difference in age distributions. This is a concern particularly for the high number of 2-year olds (the 2016 year-class) observed in May as this year-class has not been observed in any quantities in earlier cruises. It is recommended that this issue is further investigated and resolved before IESNS 2019 and also in relation to the use of these data at WGWIDE as young-fish indices.

Vertical profile across the Norwegian Sea

Two transects were taken by G.O. Sars across the whole Norwegian Sea (Figure 21). There was apparently no clear pattern in the relation between temperature and herring distribution, neither vertically nor horizontally. The herring was mainly in the western part in the temperature range of 0-6°C. Distribution of blue whiting was limited to Atlantic waters warmer than around 1.5°C (Figure 21) as also represented by its spatial distribution where it was observed across the whole Norwegian Sea except for the cold and fresh East Iceland Current (Figures 4, 5 and 18).

Mackerel

During the last decade an increasing amount of mackerel has been observed in the catches during the May survey (see last year's survey report). This pattern continued in 2018 where mackerel was caught in the central and eastern part of the Norwegian Sea (Figure 22). No quantitative information can be drawn from these data as this survey is not designed to monitor mackerel. Mackerel at age 2 (mean length 26.4 cm) was most numerous in the combined samples (not weighed by catch size), and amounted to 26 %, followed by age 1 (17 %) and age 5 (13 %).

General recommendations and comments

	RECOMMENDATION	ADRESSED TO
1.	Continue the methodological research in distinguishing between Herring and blue whiting in the interpretation of echograms.	WGIPS
2.	It is recommended that a workshop based on the ongoing otolith and scale exchange will take place before next year's IESNS survey.	WGBIOP, WGWIDE
3.	It is recommended that the WGIPS meeting in 2019 includes a workshop on how to deal with stock components of herring in the IESNS-survey.	WGIPS
4.	It is recommended that the next blue whiting otolith exchange and workshop is informed about the different age distributions observed in IESNS 2018.	WGBIOP, WGWIDE

Next year's post-cruise meeting

We will aim for next meeting in Reykjavik 18-20 June 2019. The final decision will be made at the next WGIPS meeting.

Concluding remarks

- The sea temperature in 2018 at 0-200 m depth was above long-term mean (1995-2017) in the western and central Norwegian Sea but below the mean in the eastern and southern areas of the Norwegian Sea.
- The 2018 index of meso-zooplankton biomass in the Norwegian Sea and adjoining waters decreased a bit from last year and is still comparable to the mean of the earlier high-biomass period, but is still relatively low in the westernmost areas.
- The total biomass estimate of NSSH in herring in the Norwegian Sea was 5.04 million tonnes, which is a 20 % increase from the 2017 survey estimate. The survey followed the pre-planned protocol and the survey group recommends using the abundance estimates in the analytical assessment.
- The 2013 year class dominated in the survey indices both in numbers (29 %) and biomass (25 %). Despite relatively high number at age 5 of this year class, it is half the size of the large 2004 year class at the same age.
- The estimated number at age 2 (2016 year class) of NSSH in the Barents Sea was higher in 2018 than in recent years and the fifth highest in the time series since 1991. It might indicate improved recruitment, but the uncertainty around the estimate is high.
- The biomass of blue whiting measured in the 2017 survey decreased by 46 % from last year's survey and by 54 % in number.
- Ages 2-4 (2014-2016 year classes) of blue whiting are dominating the acoustic estimate (79 % of the biomass and 78 % by numbers).

References

Foote, K. G., Knudsen, H. P., Vestnes, G., MacLennan, D. N., and Simmonds, E. J. 1987. Calibration of acoustic instruments for fish density estimation: a practical guide. ICES Coop. Res. Rep. 144: 1–57.

ICES 2009. Report of the PGNAPES Scrutiny of Echogram Workshop (WKCHOSCRU) 17–19 February 2009, Bergen, Norway ICES CM 2009/RMC

ICES. 2012. Report of the Workshop on implementing a new TS relationship for blue whiting abundance estimates (WKTSBLUES), 23–26 January 2012, ICES Headquarters, Copenhagen, Denmark. ICES CM 2012/SSGESST:01. 27 pp.

ICES. 2015. Report of the Workshop on scrutinisation procedures for pelagic ecosystem surveys (WKSCRUT), 7-11 September 2015, Hamburg, Germany. ICES CM 2015/SSGIEOM:18. 107pp.

ICES. 2016. Report of the Working Group on the Integrated Assessments of the Norwegian Sea (WGINOR), 7-11 December 2015, Reykjavik, Iceland. ICES CM 2015/SSGIEA:10. 150 pp.

ICES. 2018. Report of the Working Group on International Pelagic Surveys (WGIPS). ICES WGIPS Report 2018 15–19 January 2018. Den Helder, the Netherlands. 340 pp.

Jolly, G. M., and I. Hampton. 1990. A stratified random transect design for acoustic surveys of fish stocks. Can.J. Fish. Aquat. Sci. 47: 1282-1291.

Skjoldal, H.R., Dalpadado, P., and Dommasnes, A. 2004. Food web and trophic interactions. *In* The Norwegian Sea ecosystem. Ed. by H.R. Skjoldal. Tapir Academic Press, Trondheim, Norway: 447-506

Tables

Table 1. Survey effort by vessel for the International ecosystem survey in the Nordic Seas in May - June 2018.

Vessel	Effective survey period	Effective acoustic cruise track (nm)	Trawl stations	Ctd stations	Aged fish (HER)	Length fish (HER)	Plankton stations
Dana	05/05-25/05	1874	29	33	552	2276	32
Magnus heinason	3/5-15/5	1078	13	21	371	636	21
Árni Fridriksson	5/5-19/5	1936	22	34	1440	5502	30
G.O.Sars	03/5-1/6	3105	64	69	711	2269	76
Vilnyus	23/5-16/6	2872	28	38	314	1770	38
Total		**10865**	**156**	**195**	**3388**	**12453**	**197**

Table 2. IESNS 2018 in the Norwegian Sea. Estimates of abundance, mean weight and mean length of Norwegian spring-spawning herring.

	age																		
LenGrp	2	3	4	5	6	7	8	9	10	11	12	13	14	15	16	17	Number (1E3)	Biomass (1E3kg)	Mean W (g)
18-19	4901	-	-	-	-	-	-	-	-	-	-	-	-	-	-	-	4901	235.3	48.00
19-20	85695	-	-	-	-	-	-	-	-	-	-	-	-	-	-	-	85695	4833.2	56.40
20-21	158130	-	-	-	-	-	-	-	-	-	-	-	-	-	-	-	158130	10565.5	66.82
21-22	146523	3484	-	-	-	-	-	-	-	-	-	-	-	-	-	-	150007	11500.0	76.66
22-23	85952	83460	-	-	-	-	-	-	-	-	-	-	-	-	-	-	169413	14587.2	86.10
23-24	13243	114929	4014	-	-	-	-	-	-	-	-	-	-	-	-	-	132187	14423.5	109.12
24-25	3300	264754	-	-	-	-	-	-	-	-	-	-	-	-	-	-	268054	31519.6	117.59
25-26	1253	340495	15075	15075	-	-	-	-	-	-	-	-	-	-	-	-	371899	48523.7	130.48
26-27	-	134630	151649	5856	26710	-	-	-	-	-	-	-	-	-	-	-	318845	45809.4	143.67
27-28	-	57909	363460	92838	3951	-	-	-	-	-	-	-	-	-	-	-	518158	82561.3	159.34
28-29	-	45391	639581	219603	19358	-	1075	-	-	-	-	-	-	-	-	-	925010	160033.7	173.01
29-30	-	7173	576303	617954	27638	27418	22286	11730	4912	-	-	-	-	-	-	-	1295414	249161.7	192.34
30-31	-	-	163368	1418819	75990	36510	13054	31414	4896	-	-	-	-	-	-	-	1744050	370990.0	212.72
31-32	-	-	110460	1874863	193919	55780	34270	17217	21021	-	-	19152	-	-	-	-	2326682	540355.0	232.24
32-33	-	-	23223	1079384	248665	304970	22869	39538	7994	4958	7994	-	4958	-	-	-	1744554	435552.7	249.66
33-34	1236	-	11589	290327	195445	370623	35949	114753	-	-	14213	-	-	-	-	-	1034135	277748.2	268.58
34-35	-	-	4491	65698	132898	406123	122429	197401	22242	40719	105839	43229	49154	-	7983	-	1198205	351759.3	293.57
35-36	-	-	-	5969	48754	182479	231490	441721	93455	240023	434621	334872	221419	18106	14485	-	2267395	707529.2	312.04
36-37	-	-	-	-	-	48699	76399	312391	65597	262479	585867	594494	601101	83594	19622	-	2650243	868235.6	327.61
37-38	-	-	-	-	-	985	-	130688	117576	119672	366092	437464	429959	124381	59389	16747	1802952	622166.4	345.08
38-39	-	-	-	-	-	-	1128	31348	-	20976	39777	36864	206505	25287	54441	11123	427448	157798.9	369.16
39-40	-	-	-	-	-	-	-	-	-	-	5487	11761	15571	6415	37895	8553	85681	33928.4	395.98
40-41	-	-	-	-	-	-	-	-	-	-	4799	-	-	-	-	-	4799	1842.7	384.00
TSN(1000)	500232	1052226	2063214	5686387	973329	1433588	560950	1328201	337692	688827	1564688	1477836	1528668	257783	193815	36423	19683857	-	-
TSB(1000 kg)	36405.6	133291.7	374152.3	1275393.0	240593.2	393848.5	163141.4	405473.4	108056.1	223975.1	506171.3	490108.9	518277.3	89915.9	69296.3	13560.6	-	5041660.7	-
Mean length (cm)	20.86	24.90	28.54	30.83	32.09	33.38	34.25	35.01	35.49	35.82	35.96	36.06	36.44	36.70	37.40	37.78	-	-	-
Mean weight (g)	72.78	126.68	181.34	224.29	247.19	274.73	290.83	305.28	319.98	325.15	323.50	331.64	339.04	348.80	357.54	372.31	-	-	256.13

Table 3. IESNS 2018 in the Barents Sea. Estimates of abundance, mean weight and mean length of Norwegian spring-spawning herring.

	age							
LenGrp	1	2	3	4	Unknown	Number (1E3)	Biomass (1E3kg)	Mean W (g)
8-9	-	-	-	-	520041	520041	-	-
9-10	1387351	-	-	-	-	1387351	6705.5	4.83
10-11	3454174	-	-	-	-	3454174	23047.7	6.67
11-12	1729698	-	-	-	-	1729698	14235.4	8.23
12-13	87114	580761	-	-	-	667875	7482.1	11.20
13-14	55348	525809	-	-	-	581157	8302.2	14.29
14-15	152238	418656	-	-	-	570894	9971.6	17.47
15-16	-	2482188	-	-	-	2482188	55037.4	22.17
16-17	-	4567488	-	-	-	4567488	118814.1	26.01
17-18	-	3502545	-	-	-	3502545	108991.0	31.12
18-19	-	752673	-	-	-	752673	27545.4	36.60
19-20	-	1795332	96523	-	-	1891855	90606.3	47.89
20-21	-	1583094	98943	-	-	1682038	89929.6	53.46
21-22	-	1003720	54748	-	-	1058468	66592.3	62.91
22-23	-	118952	288884	-	-	407836	32057.6	78.60
23-24	-	72411	90513	-	-	162924	14029.6	86.11
24-25	-	-	78268	-	-	78268	8609.4	110.00
25-26	-	-	235335	-	-	235335	25886.9	110.00
27-28	-	-	-	9227	-	9227	1324.0	143.50
TSN(1000)	6865924	17403628	943215	9227	520041	25742035	-	-
TSB(1000 kg)	48040.8	581618.4	78185.0	1324.0	-	-	709168.2	-
Mean length (cm)	10.47	17.15	22.56	27.50	8.50	-	-	-
Mean weight (g)	7.00	33.42	82.89	143.50	-	-	-	28.12

Table 4. IESNS 2018 in the Norwegian Sea. Estimates of abundance, mean weight and mean length of blue whiting.

LenGrp	age 1	2	3	4	5	6	7	8	9	10	11	12	13	Unknown	Number (1E3)	Biomass (1E3kg)	Mean W (g)
18-19	13911	-	-	-	-	-	-	-	-	-	-	-	-	-	13911	514.7	37.00
19-20	26636	-	-	-	-	-	-	-	-	-	-	-	-	-	26636	1017.3	38.19
20-21	85769	-	-	-	-	-	-	-	-	-	-	-	-	-	85769	3861.8	45.03
21-22	86969	21591	317	-	-	-	-	-	-	-	-	-	-	-	108877	5699.8	52.35
22-23	163191	12543	1775	-	-	-	-	-	-	-	-	-	-	-	177509	10463.4	58.95
23-24	35165	74535	11626	4550	-	-	-	-	-	-	-	-	-	-	125877	8951.7	71.11
24-25	23535	244175	56159	28210	2135	-	-	-	-	-	-	-	-	-	354214	29602.1	83.57
25-26	4253	402575	145174	92393	10188	-	-	-	-	-	-	-	-	-	654582	62861.3	96.03
26-27	-	377994	190087	290411	31258	5288	-	-	-	-	-	-	-	-	895039	96981.5	108.35
27-28	1523	246510	144361	374003	97499	9521	536	473	-	-	-	-	-	-	874427	105639.2	120.81
28-29	-	76062	113124	222973	98111	17506	6333	-	-	-	-	-	-	-	534109	72406.0	135.56
29-30	-	28914	66980	119522	70636	16462	786	-	-	-	-	-	-	-	303301	45879.0	151.27
30-31	-	1601	37824	40757	35577	19888	2152	-	-	-	-	4802	-	-	142601	23623.1	165.66
31-32	-	3092	19574	8698	11874	10844	8952	-	6162	-	-	-	-	-	69196	12883.5	186.19
32-33	-	1593	15935	517	4413	4449	2979	-	-	-	-	-	-	-	29887	5881.4	196.79
33-34	-	-	-	-	8513	1860	18361	1240	1240	-	-	-	-	-	31215	6365.6	203.93
34-35	-	-	-	1614	-	2599	1818	3898	-	-	-	-	-	-	9929	2453.5	247.11
35-36	-	-	-	1370	-	-	4316	1439	1023	1439	-	-	-	-	9585	2615.7	272.89
36-37	-	-	-	-	-	574	287	-	559	-	1119	-	-	-	2539	668.5	263.25
37-38	-	-	-	-	-	-	-	-	-	-	-	-	-	849	849	274.9	323.70
38-39	-	-	-	-	-	-	-	-	763	-	-	-	763	-	1526	498.1	326.50
39-40	-	-	-	-	-	-	-	-	-	-	-	-	-	-	-	-	-
41-42	-	-	-	4605	-	-	-	-	-	-	-	-	-	-	4605	1510.4	328.00
TSN(1000)	440951	1491186	802935	1189624	370205	88991	46520	7050	9747	1439	1119	4802	763	849	4456182	-	-
TSB(1000 kg)	24407.6	152104.0	96146.8	146812.4	51564.3	14525.5	9174.7	1659.5	2167.6	388.4	298.2	858.0	270.8	274.9	-	500652.6	-
Mean length (cm)	21.45	25.53	26.92	27.29	28.28	29.50	31.98	33.70	32.68	35.00	36.00	30.17	38.00	37.38	-	-	-
Mean weight (g)	55.35	102.00	119.74	123.41	139.29	163.22	197.22	235.40	222.38	270.00	266.50	178.67	355.00	323.70	-	-	112.35

Figures

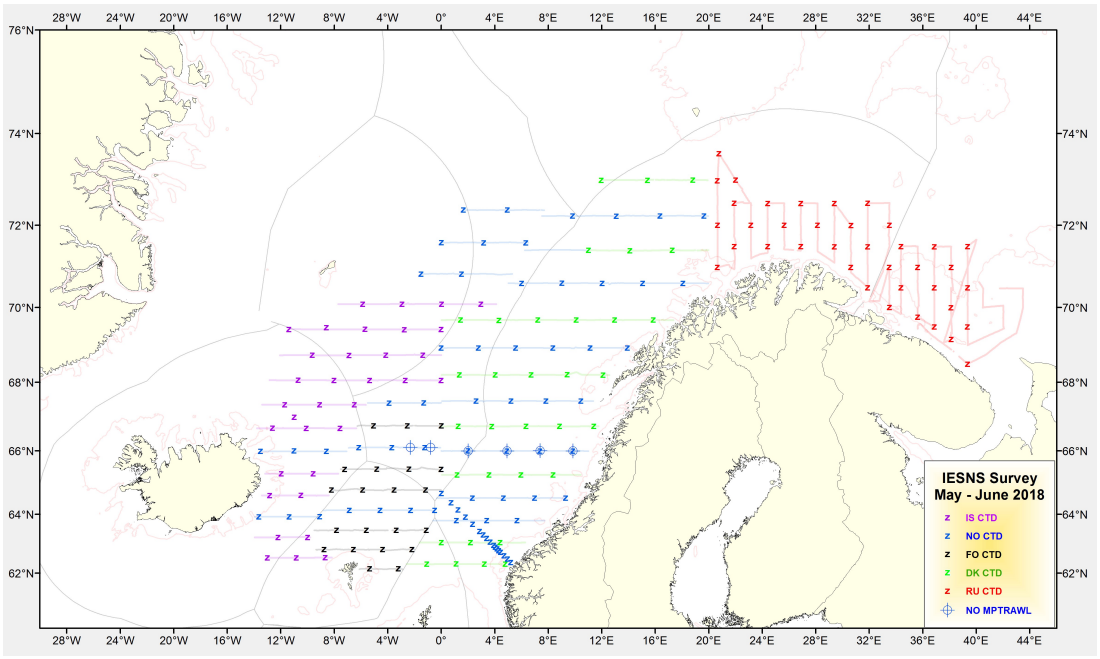

Figure 1. Cruise tracks and CTD stations by country for the IESNS survey in May-June 2018. Manta trawl hauls for sampling of micro plastics in the surface are also shown.

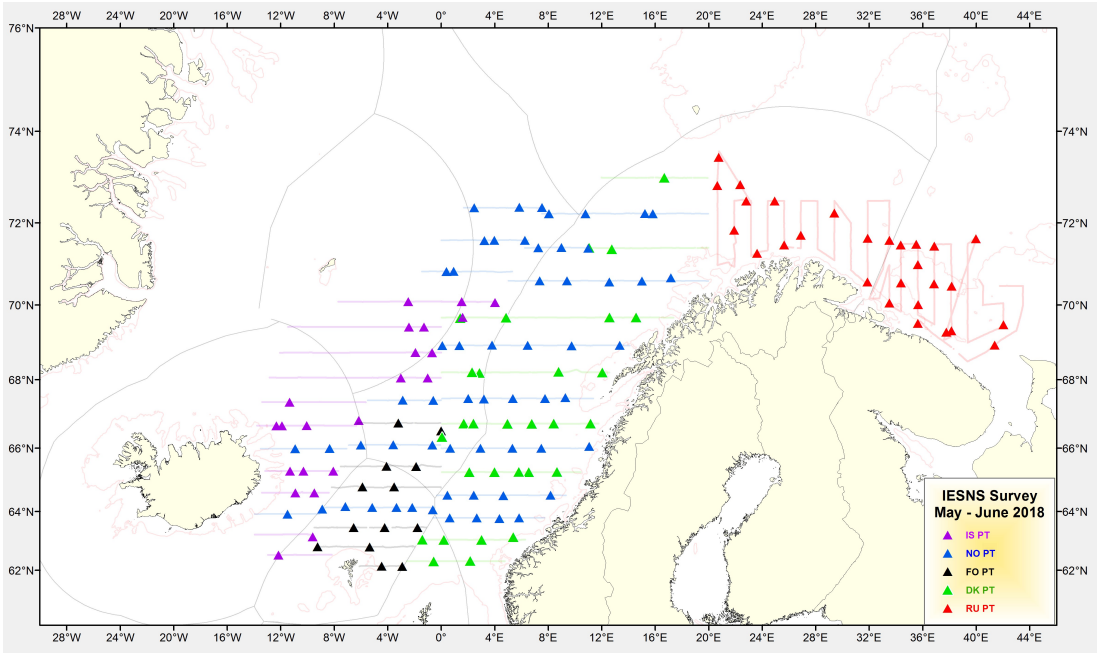

Figure 2. Cruise tracks during the IESNS survey in May-June 2018 and location of trawl stations.

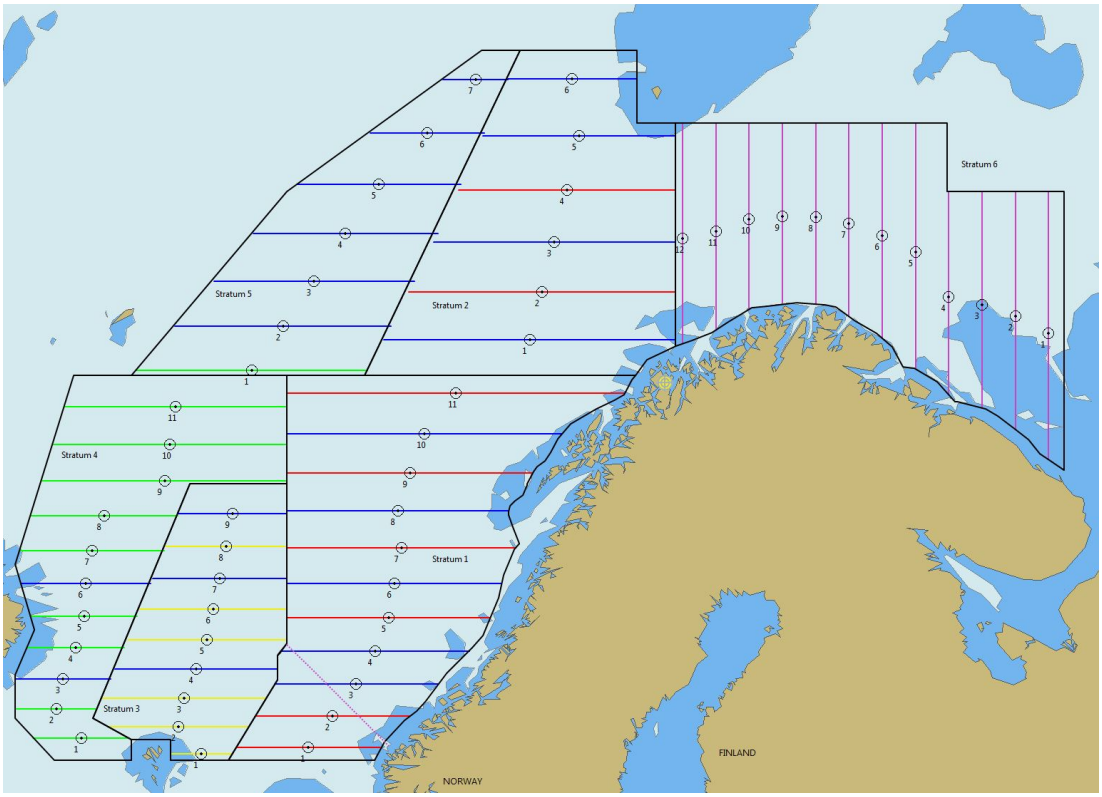

Figure 3. The pre-planned strata and transects for the IESNS survey in 2018 (red: EU, dark blue: Norway, yellow: Faroes Islands, violet: Russia, green: Iceland).

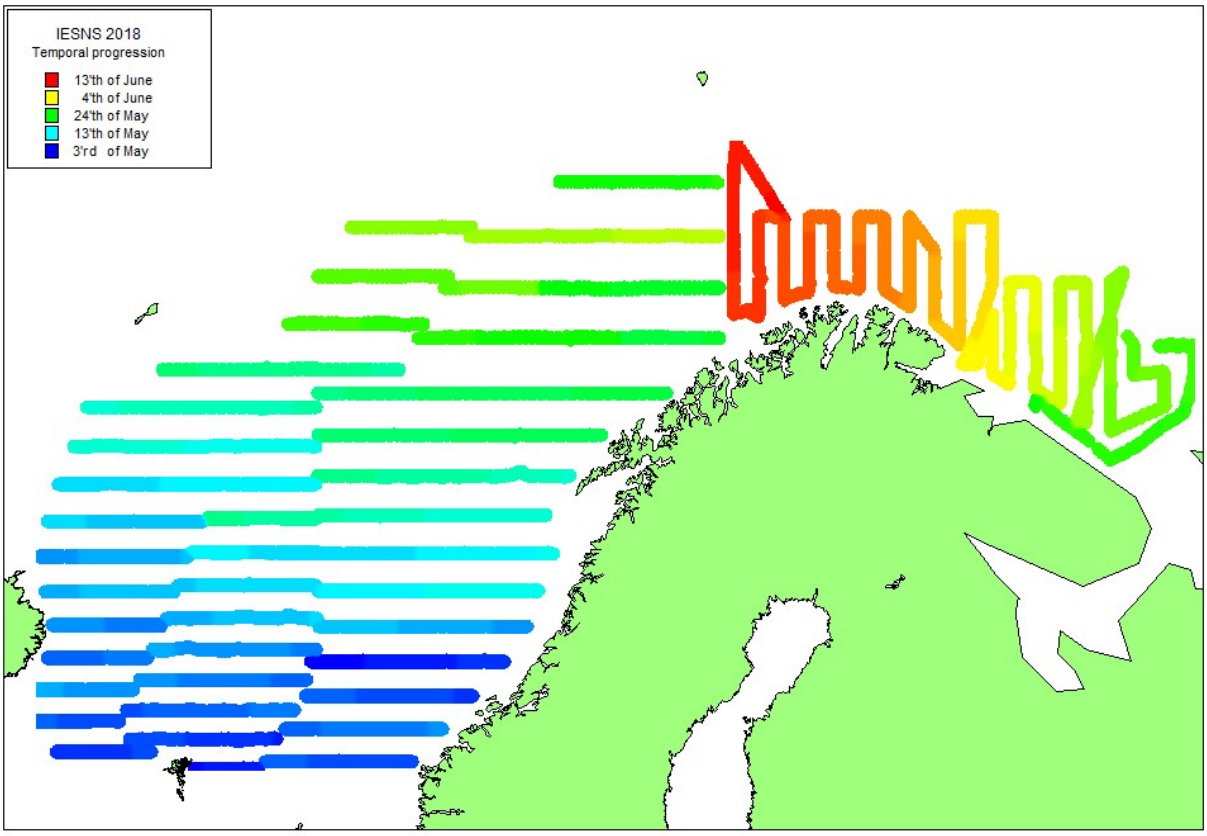

Figure 4. Temporal progression IESNS in May-June 2018.

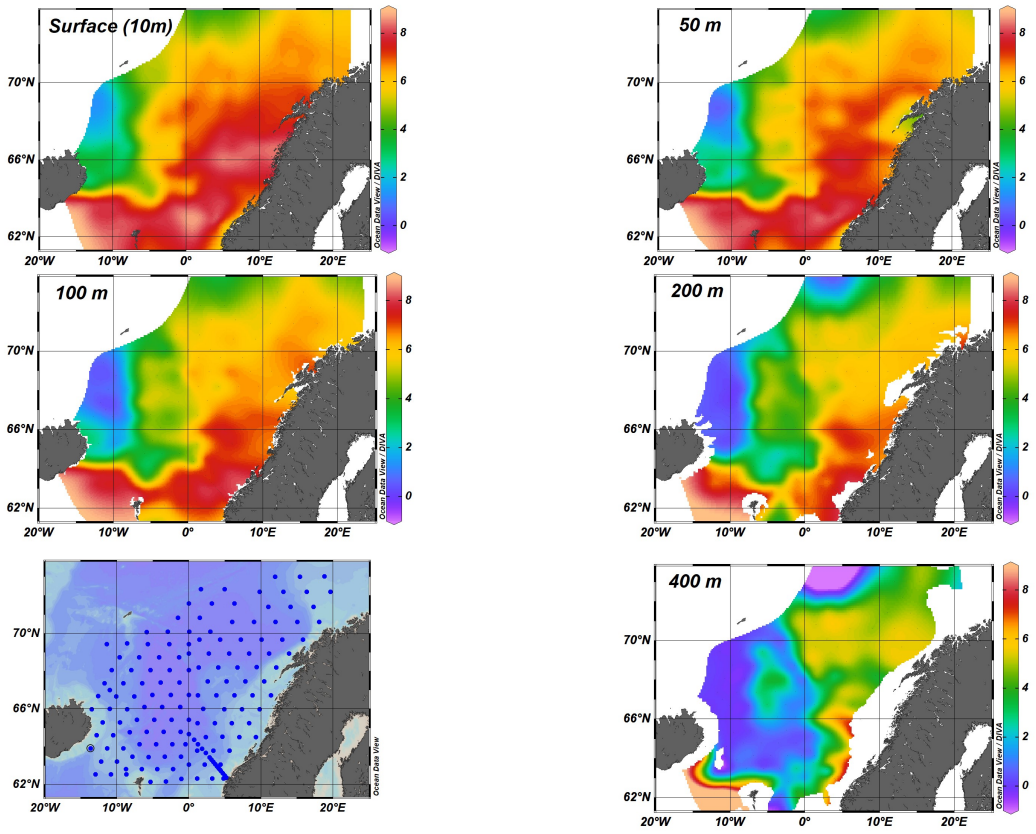

Figure 5. The horizontal distribution of temperatures (°C) at 10 m (surface), 50m, 100m, 200m and 400m depth in IESNS in May-June 2018.

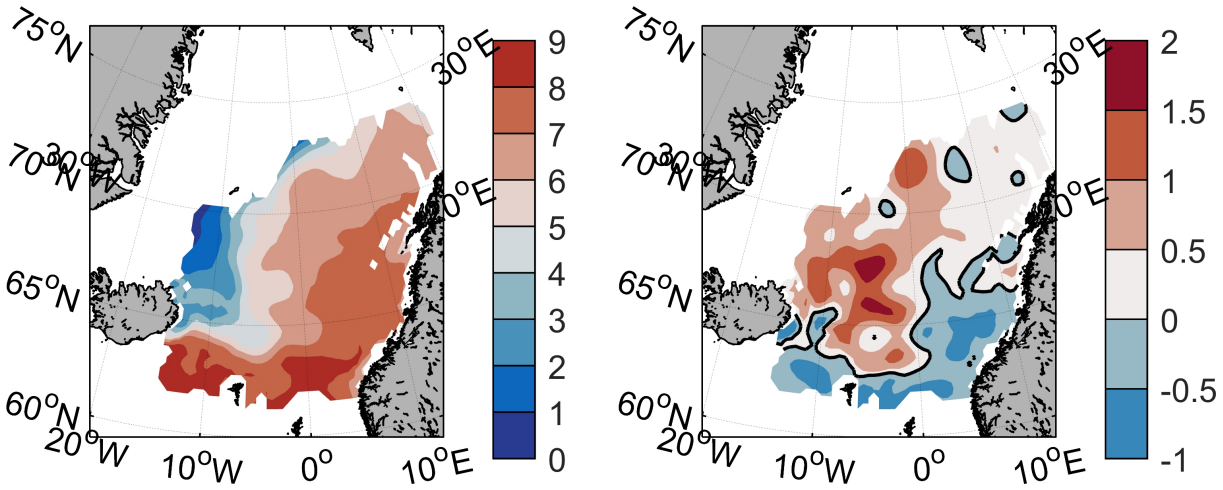

Figure 6. Temperature (left) and temperature anomaly (right) averaged over 0-50 m depth in May 2018. Anomaly is relative to the 1995-2017 mean.

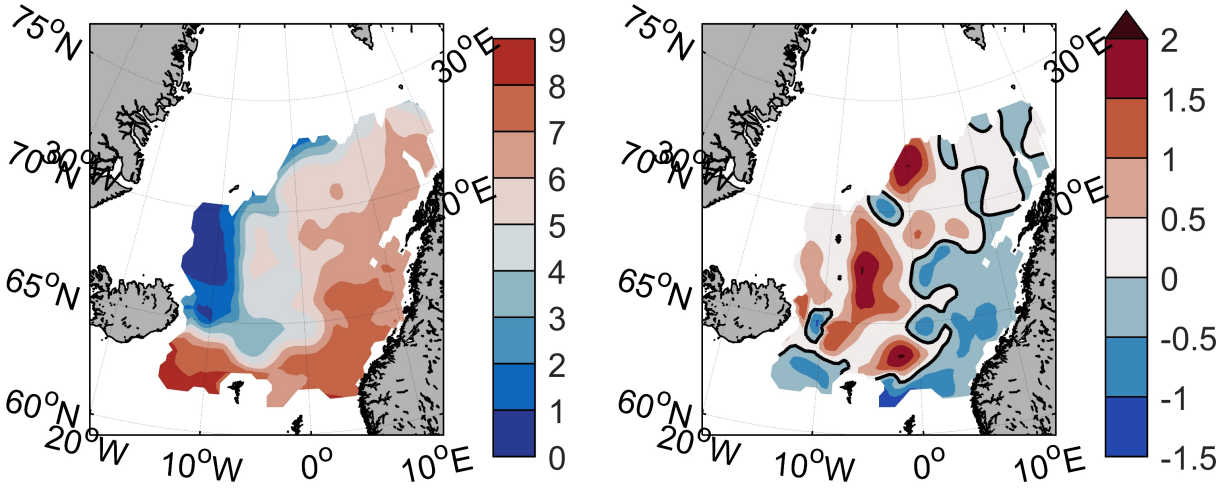

Figure 7. Temperature (left) and temperature anomaly (right) averaged over 50-200 m depth in May 2018. Anomaly is relative to the 1995-2017 mean.

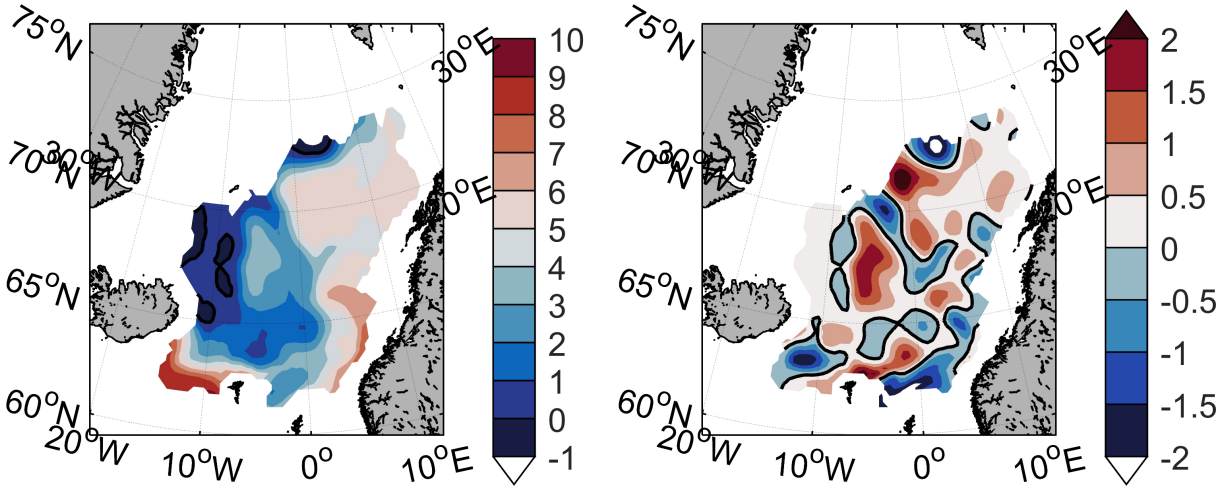

Figure 8. Temperature (left) and temperature anomaly (right) averaged over 200-500 m depth in May 2018. Anomaly is relative to the 1995-2017 mean.

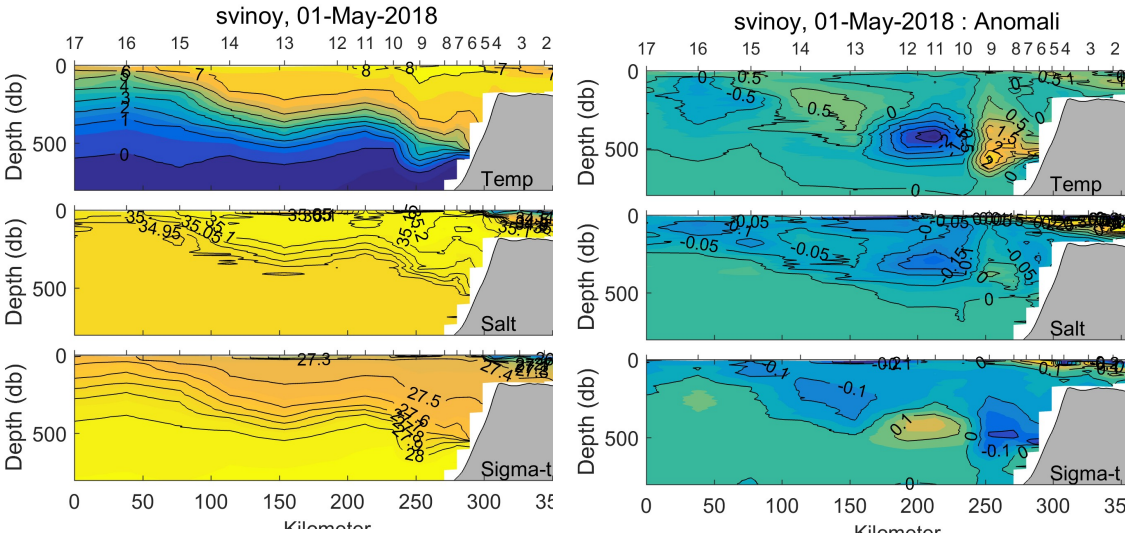

Figure 9. Temperature, salinity and potential density (sigma-t) (left hand panel) and anomalies (right hand panel) at the Svinøy section, May 2018. Anomalies are relative to a 30 years long-term mean (1978-2007).

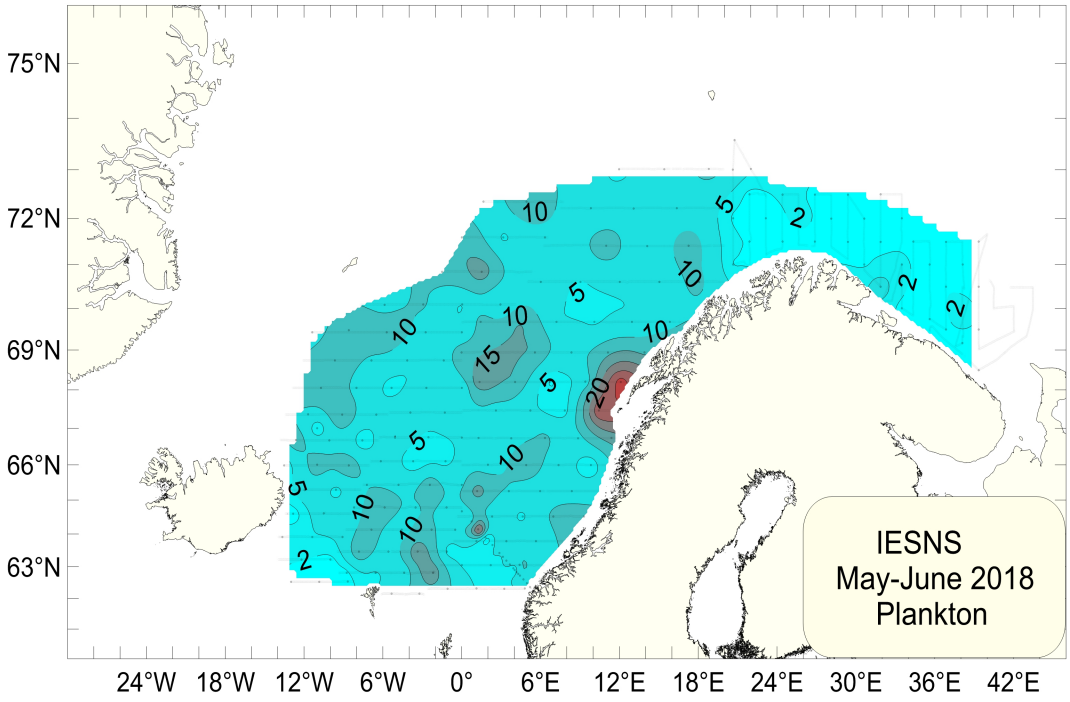

Figure 10. Representation of zooplankton biomass (g dry weight m^{-2}; at 0-200 m depth) in May-June 2018.

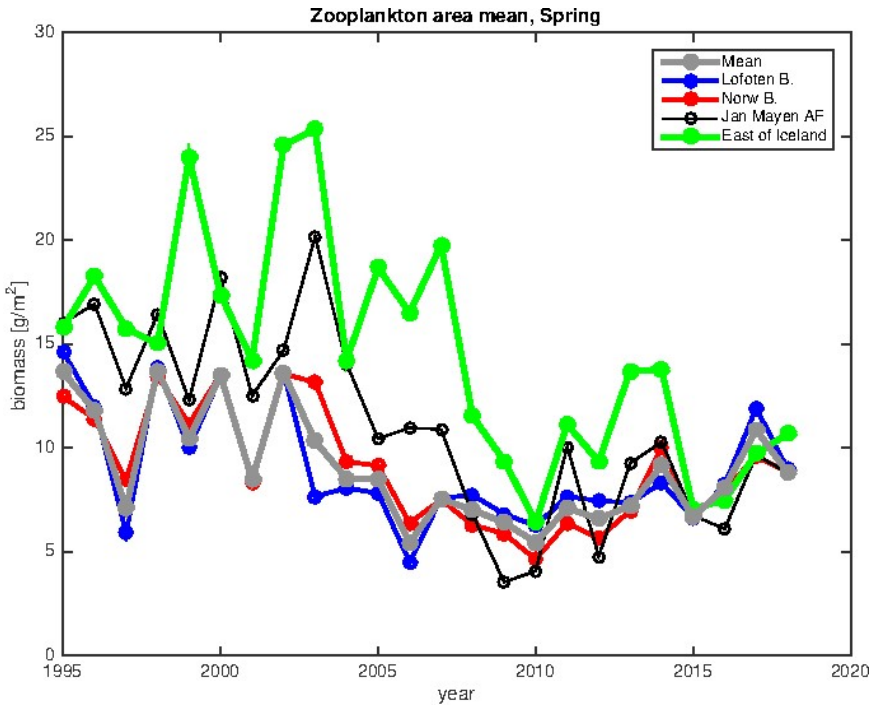

Figure 11. Indices of zooplankton dry weight (g m^{-2}) sampled by WP2 in May in (a) the different areas in and near Norwegian Sea from 1997 to 2018 as derived from interpolation using objective analysis utilizing a Gaussian correlation function (see details on methods and areas in ICES 2016).

(a)

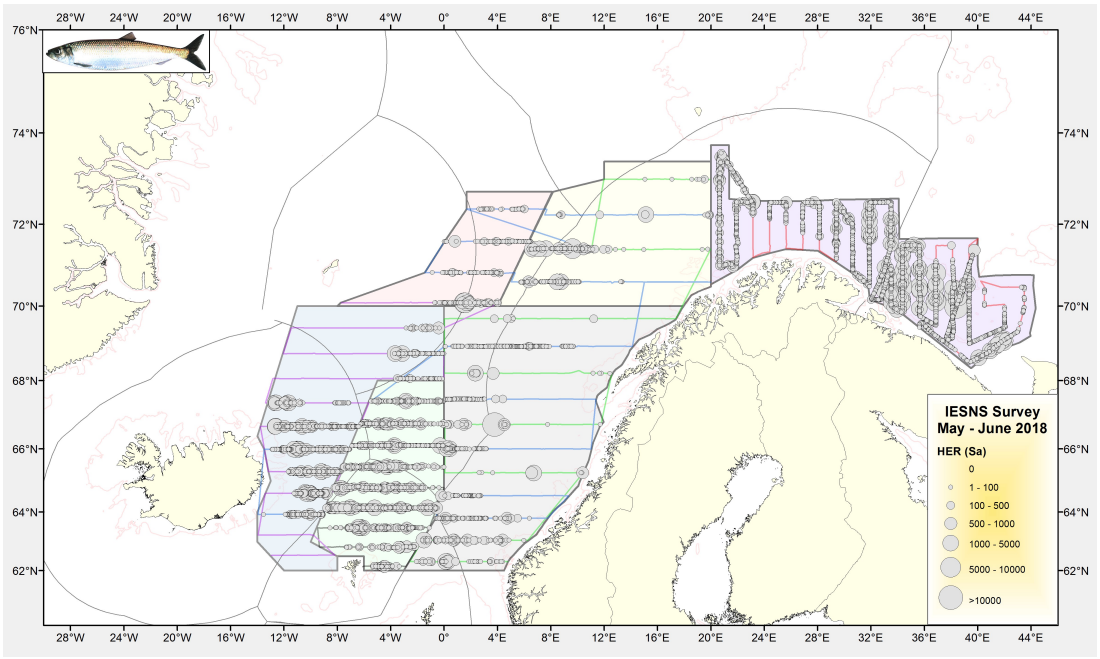

(b)

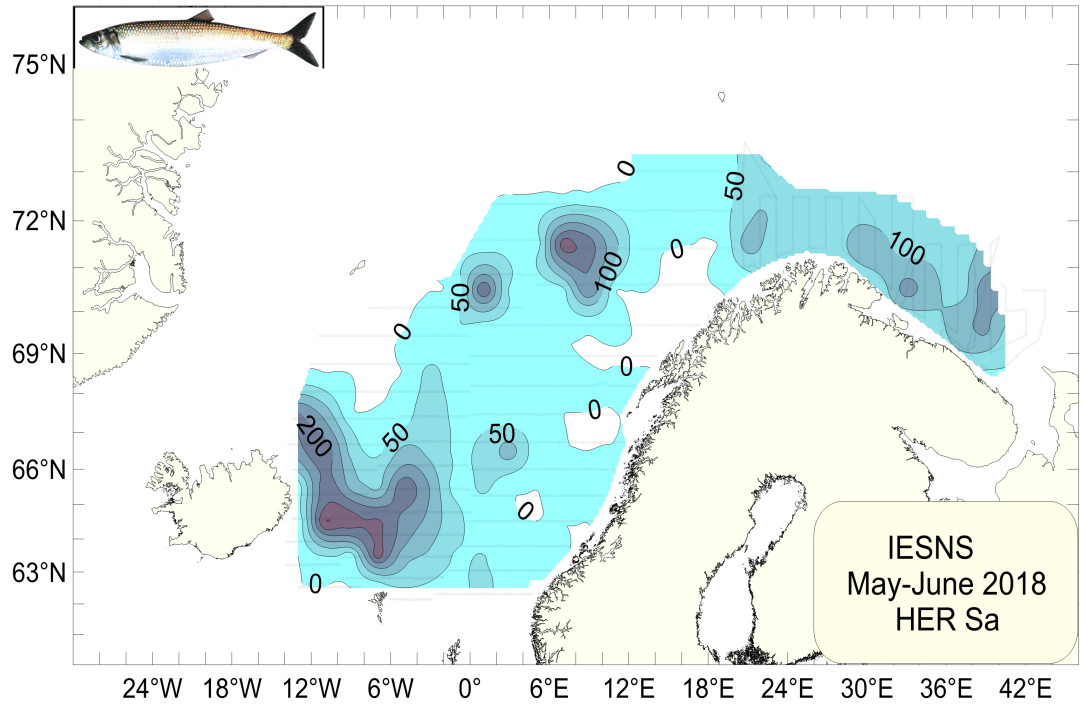

Figure 12. Distribution of Norwegian spring-spawning herring as measured during the IESNS survey in April-June 2018 in terms of NASC values (m²/nm²) (a) averaged for every 1 nautical mile and (b) represented by a contour plot. The stratification of the survey area is shown on the upper map.

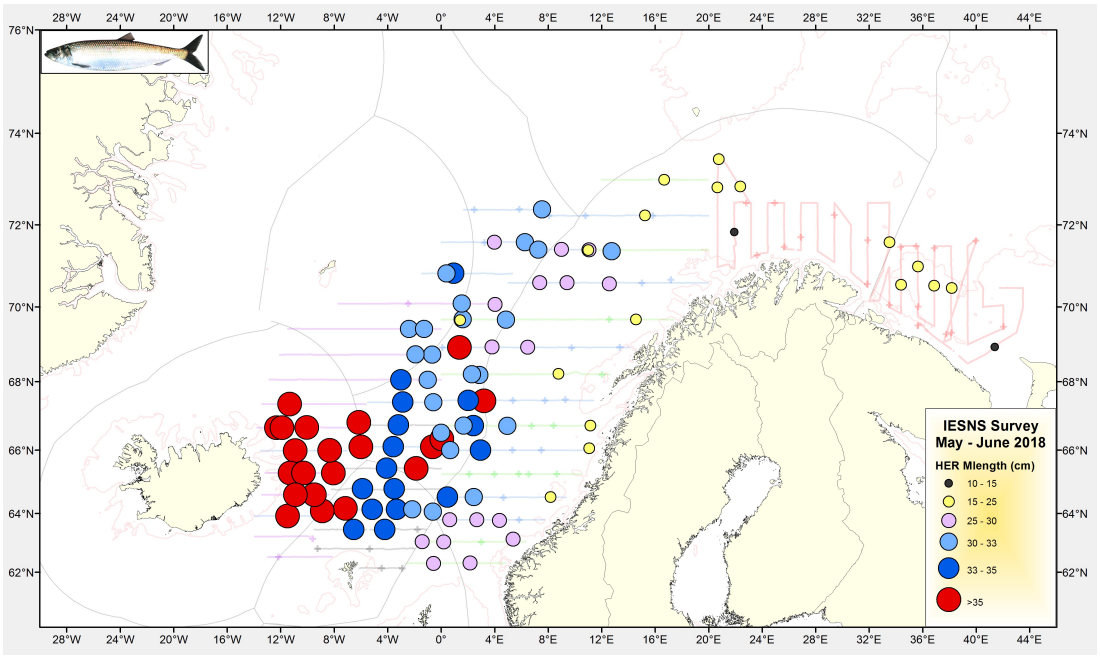

Figure 13. Mean length of Norwegian spring-spawning herring in all hauls in April-June 2018.

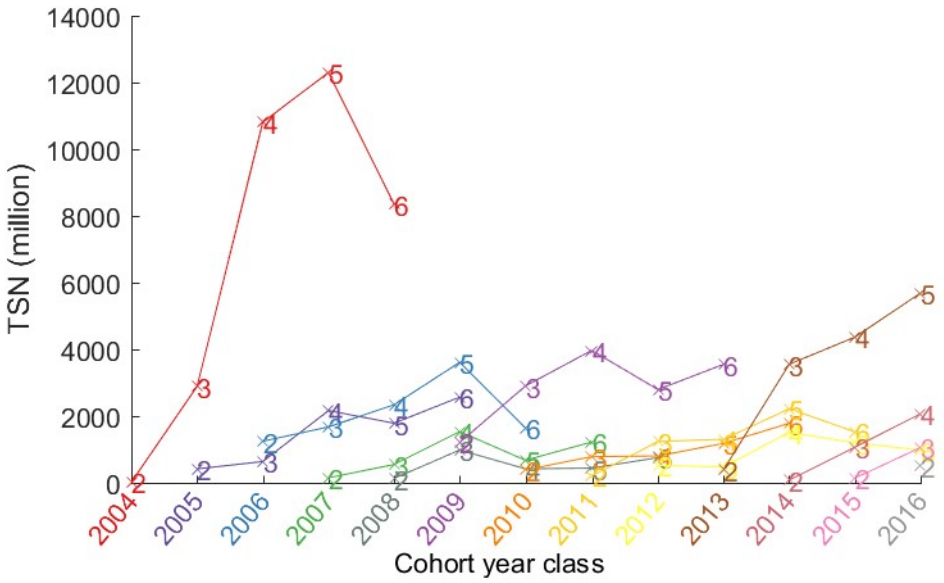

Figure 14. Tracking of the Total Stock Number (TSN, in millions) of Norwegian spring-spawning herring for each cohort since 2004 from age 2 to age 6. From 2008, stock is estimated using the StoX software. Prior to 2008, stock was estimated using BEAM.

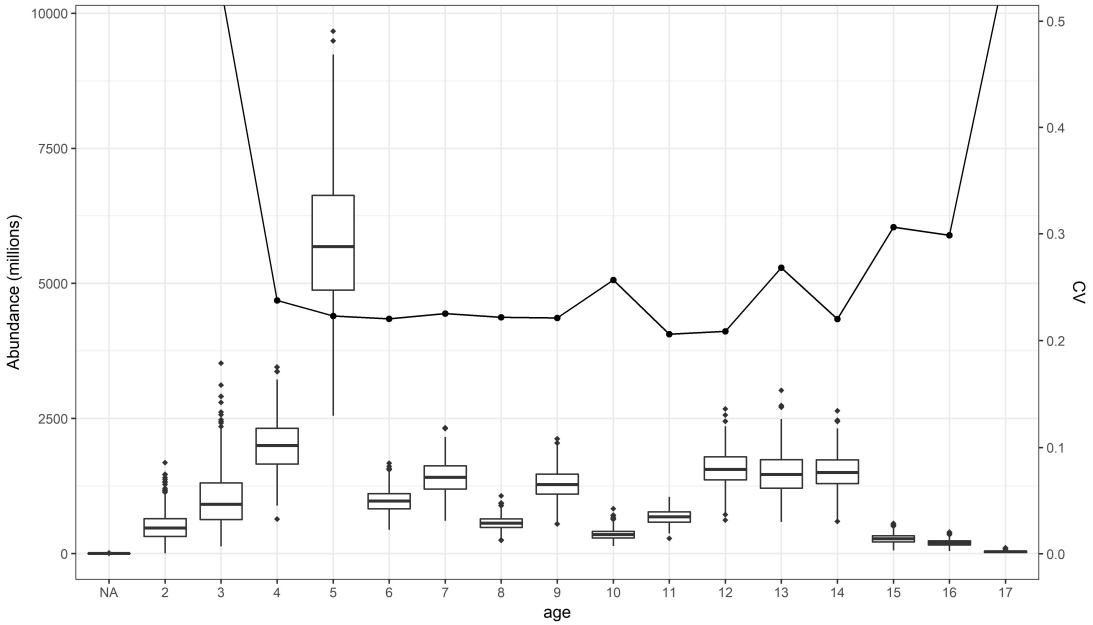

Figure 15. Norwegian spring-spawning herring in the Norwegian Sea: R boxplot of abundance and relative standard error (CV) obtained by bootstrapping with 500 replicates using the StoX software.

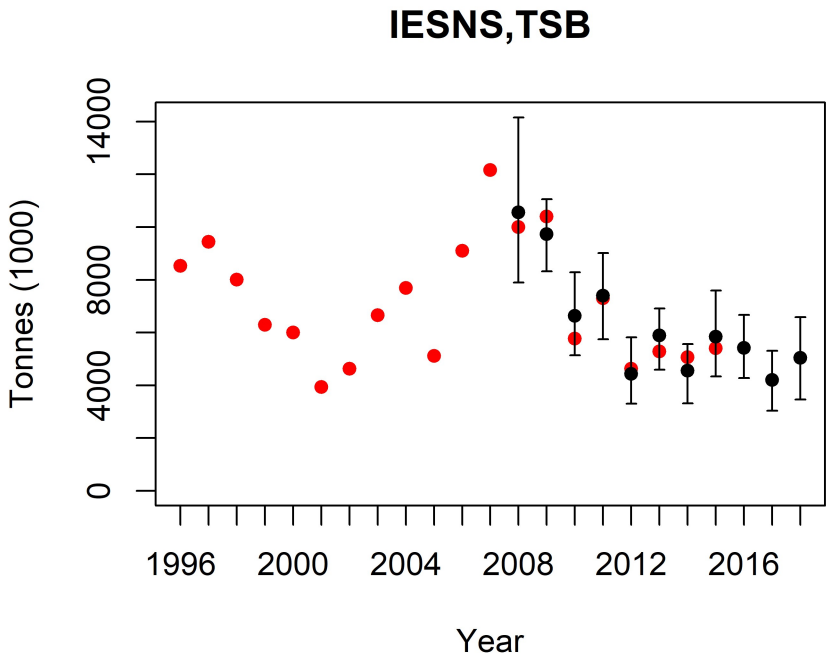

Figure 16. The annual biomass index of Norwegian-spring spawning herring in the IESNS survey (Barents Sea, east of 20°E, is excluded) from 1996 to 2018 as estimated using BEAM (red dots; calculated on basis of rectangles) and as estimated with the software StoX (black dots with 90% confidence interval; calculated on basis of standard stratified transect design).

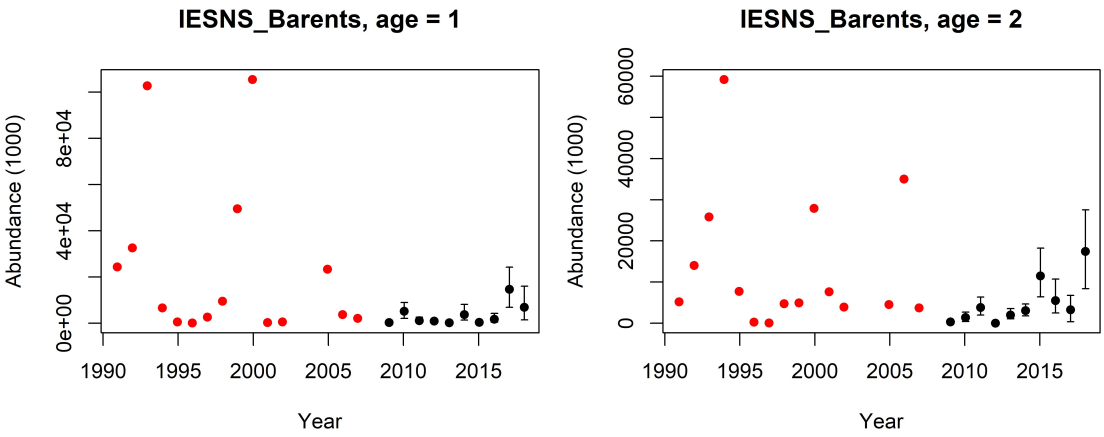

Figure 17. Numbers at age 1 (to left) and age 2 (right) herring in the Barents Sea in April-June as estimated using BEAM (red dots; calculated on basis of rectangles) and the software StoX (black dots with 90% confidence interval; calculated on basis of standard stratified transect design).

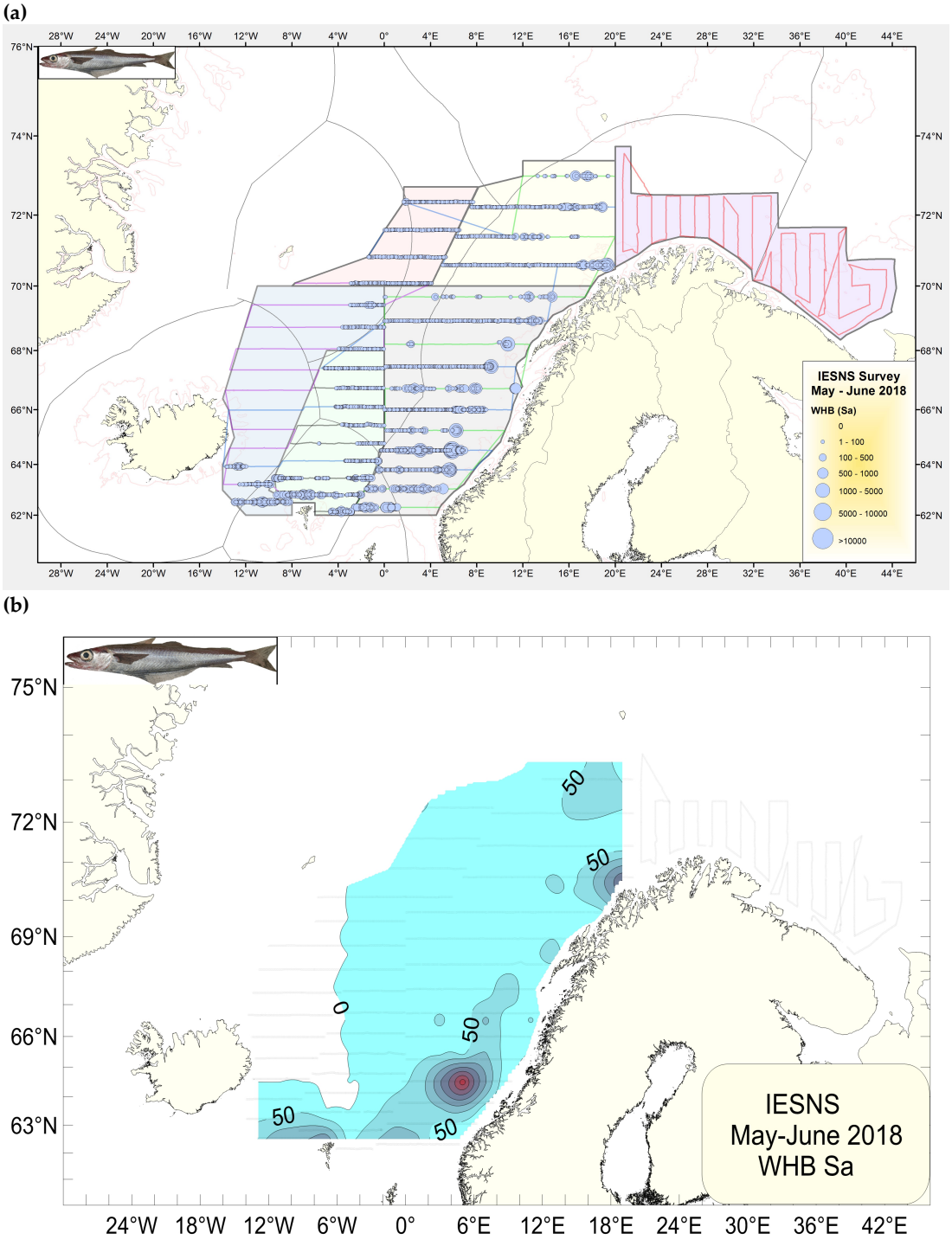

Figure 18. Distribution of blue whiting as measured during the IESNS survey in April-June 2018 in terms of NASC values (m²/nm²) (a) averaged for every 1 nautical mile and (b) represented by a contour plot. The stratification of the survey area is shown on the upper map.

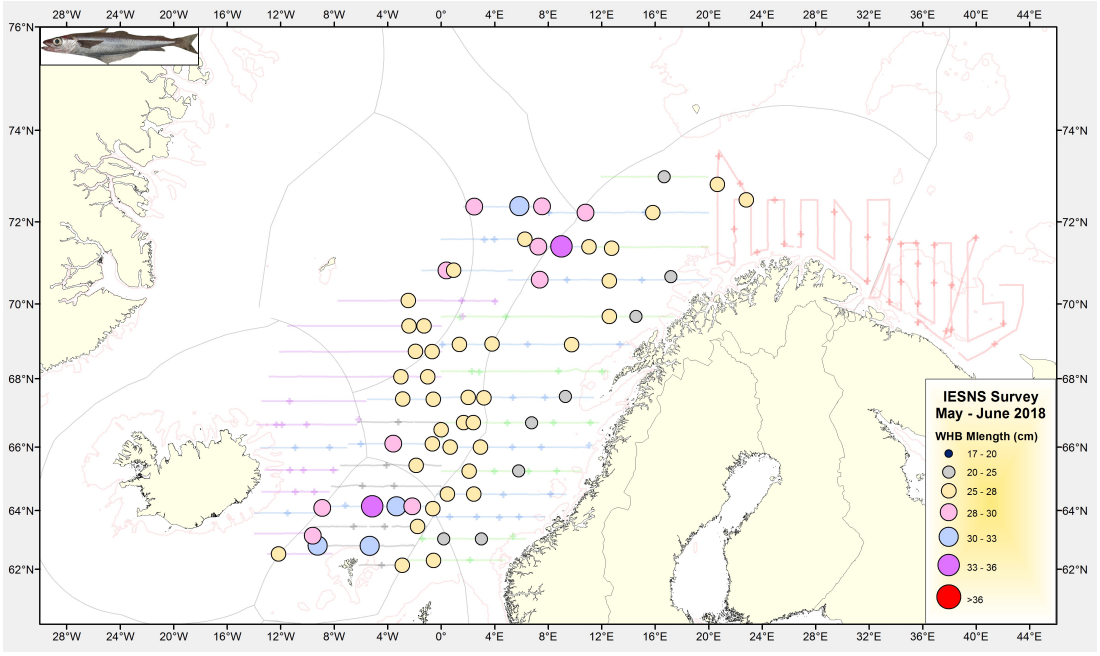

Figure 19. Mean length of blue whiting in all hauls in IESNS 2018.

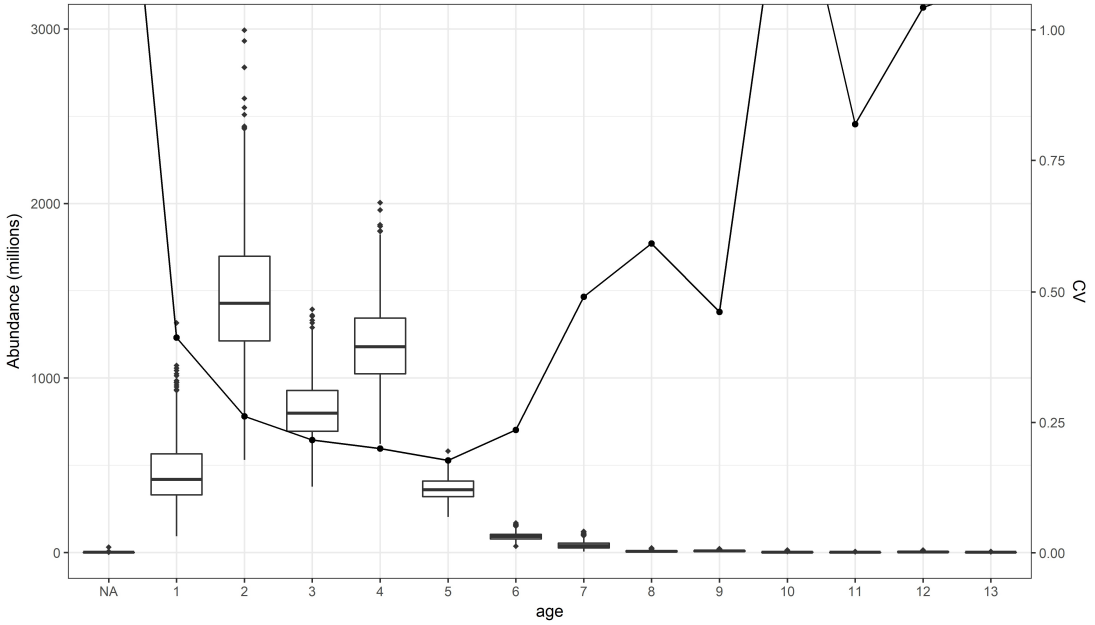

Figure 20. Blue whiting in the Norwegian Sea: R boxplot of abundance and relative standard error (CV) obtained by bootstrapping with 500 replicates using the StoX software.

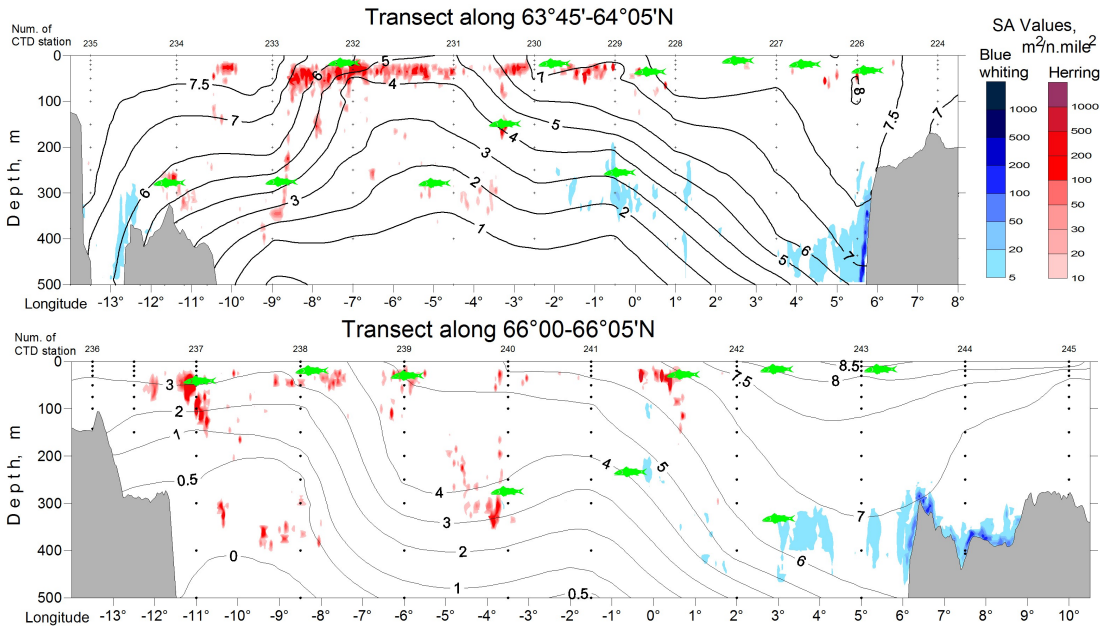

Figure 21. Acoustic values of NSS-herring (red) and blue whiting (blue), location of trawl stations (green fish) and temperature profile (black lines) along two transects across the whole Norwegian Sea in May 2018, covered by "G.O. Sars".

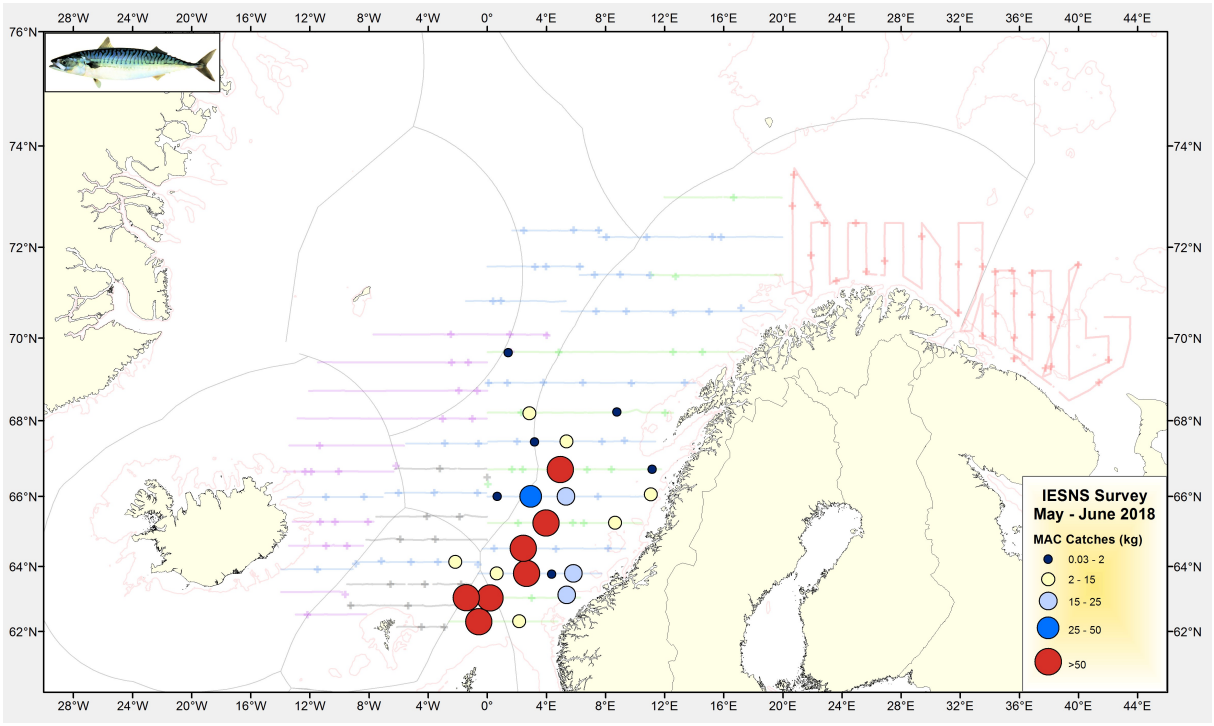

Figure 22. Distribution of hauls containing mackerel and the catch size in the 2018 IESNS.

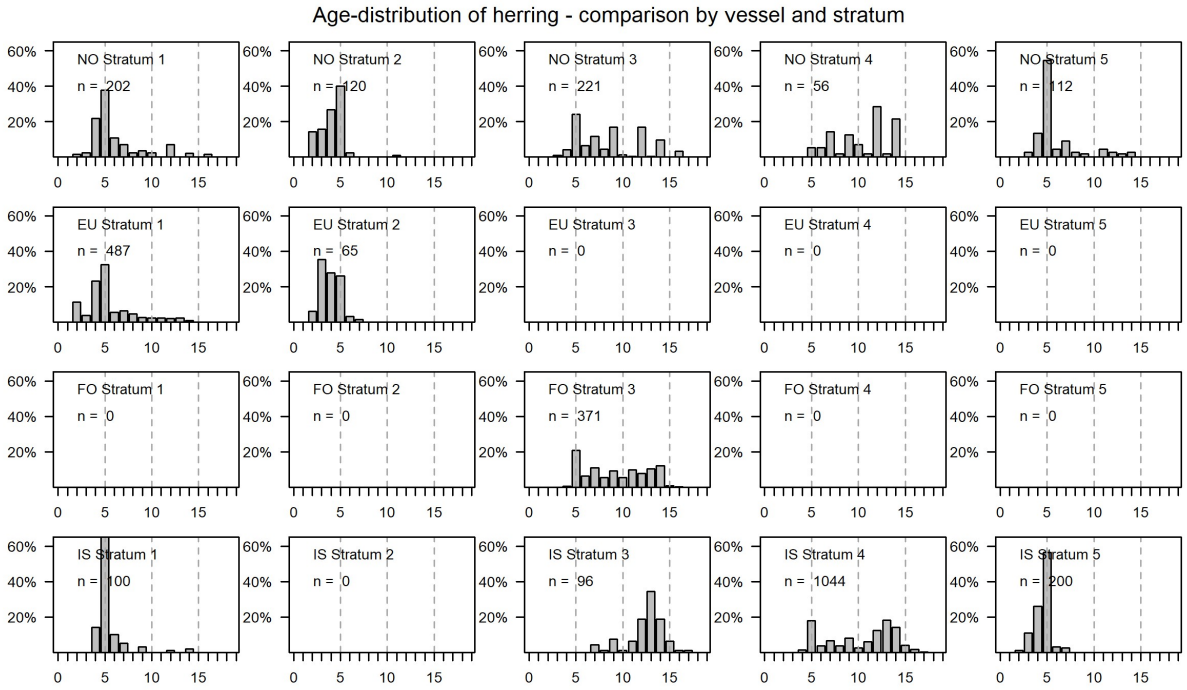

Figure 23. Comparison of the age distributions of NSS-herring by stratum and country in IESNS 2018. The strata are shown in Figure 3.

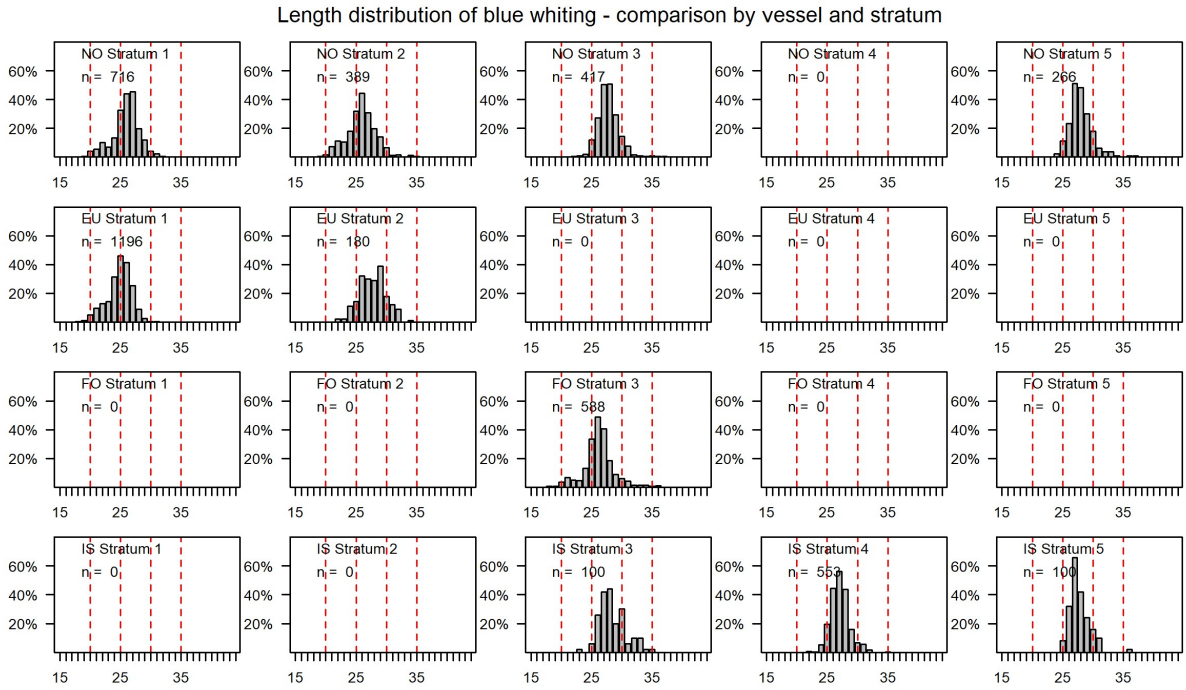

Figure 24. Comparison of the length distributions of blue whiting by stratum and country in IESNS 2018. The strata are shown in Figure 3.

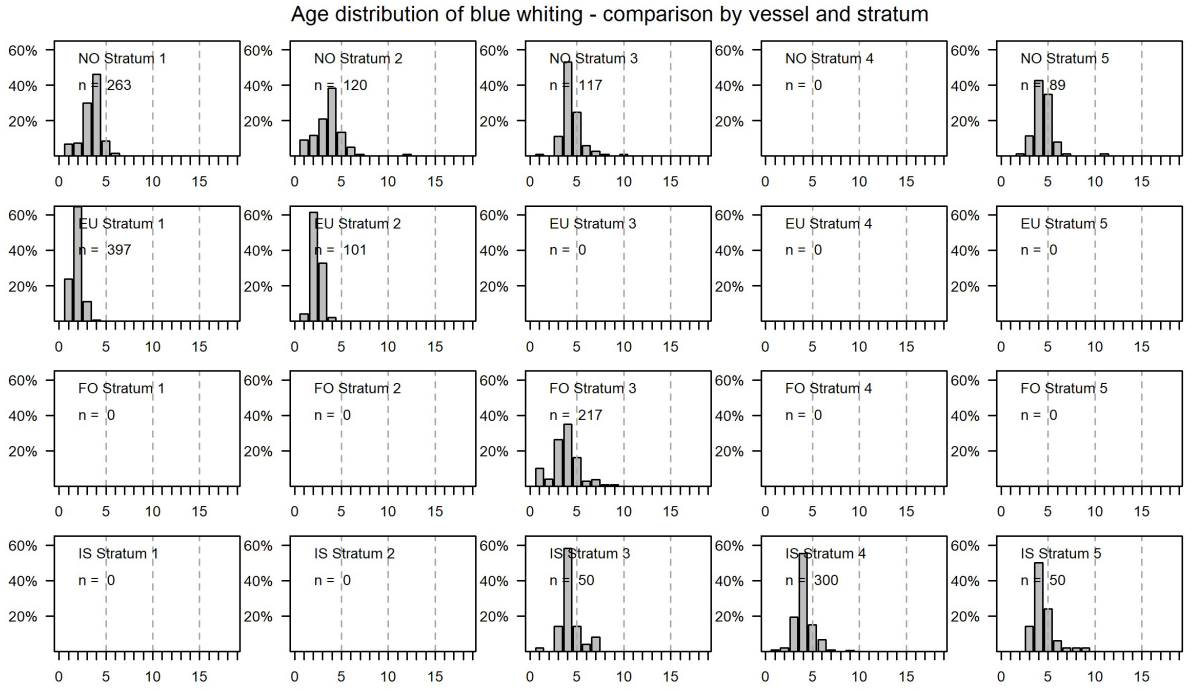

Figure 25. Comparison of the age distributions of blue whiting by stratum and country in IESNS 2018. The strata are shown in Figure 3.

Appendix 1

Corrected estimates for IESNS 2017

When the stox estimates for 2017 was obtained at the post-cruise meeting in Bergen in june 2017 an error was made: the biological data from the Norwegian vessel was omitted. This error was discovered recently, and at the IESNS post-cruise meeting in June 2018 it was decided to present the corrected estimates (i.e. with the Norwegian biological data included in the stox estimate) as an appendix to the IESNS 2018 cruise report. The corrected point estimates for Norwegian spring-spawning herring are shown in table A1 and figure A1. The corrected estimates are quite similar to the original estimates, the most notable difference is higher corrected estimate of the abundance of 13 year old herring (2004 year class). The corrected point estimates for blue whiting are shown in table A2 and Figure A2. The differences between the original and corrected estimates are very small. Based on the confidence intervals obtained from boostrap runs in Stox the corrected and original herring and blue whiting estimates of abundance at age are not significantly different from the original estimates (results not shown here).

Table A1. IESNS 2017 in the Norwegian Sea. Corrected estimates of abundance, mean weight and mean length of Norwegian spring-spawning herring.

LenGrp	age 1	2	3	4	5	6	7	8	9	10	11	12	13	14	15	16	18	Unknown	Number (1E3)	Biomass (1E3kg)	Mean W (g)
11-12	5622	-	-	-	-	-	-	-	-	-	-	-	-	-	-	-	-	-	5622	45.0	8.00
12-13	-	-	-	-	-	-	-	-	-	-	-	-	-	-	-	-	-	5622	5622	50.6	9.00
13-14	-	-	-	-	-	-	-	-	-	-	-	-	-	-	-	-	-	5622	5622	78.7	14.00
14-15	-	-	-	-	-	-	-	-	-	-	-	-	-	-	-	-	-	-	-	-	-
15-16	5116	-	-	-	-	-	-	-	-	-	-	-	-	-	-	-	-	-	5116	133.0	26.00
16-17	-	-	-	-	-	-	-	-	-	-	-	-	-	-	-	-	-	-	-	-	-
17-18	-	-	-	-	-	-	-	-	-	-	-	-	-	-	-	-	-	-	-	-	-
18-19	-	-	-	-	-	-	-	-	-	-	-	-	-	-	-	-	-	1843	1843	88.5	48.00
19-20	-	8334	-	-	-	-	-	-	-	-	-	-	-	-	-	-	-	-	8334	432.4	51.88
20-21	-	25615	-	-	-	-	-	-	-	-	-	-	-	-	-	-	-	-	25615	1440.9	56.25
21-22	-	31343	-	-	-	-	-	-	-	-	-	-	-	-	-	-	-	-	31343	2169.7	69.22
22-23	-	23895	48155	6338	-	-	-	-	-	-	-	-	-	-	-	-	-	-	78389	6372.9	81.30
23-24	-	15794	128944	15794	3949	-	-	-	-	-	-	-	-	-	-	-	-	-	164481	14930.2	90.77
24-25	-	-	275215	10219	-	3172	-	-	-	-	-	-	-	-	-	-	-	-	288607	29974.9	103.86
25-26	-	-	250725	57680	-	-	-	-	-	-	-	-	-	-	-	-	-	-	308405	35701.5	115.76
26-27	-	-	95647	361602	-	-	-	-	-	-	-	-	-	-	-	-	-	-	457248	59474.1	130.07
27-28	-	3452	36491	715828	94399	3452	-	-	9530	-	-	-	-	-	-	-	-	-	863152	130151.1	150.79
28-29	-	-	101646	1255870	241522	61454	30373	9991	4996	-	18805	-	-	-	-	-	-	-	1724657	288039.2	167.01
29-30	-	23669	69301	1172540	309389	102965	100807	38078	55000	4298	8595	-	-	-	-	-	-	-	1885240	342156.3	181.49
30-31	-	-	15983	529572	249850	327652	213289	157136	23963	9585	4793	1739	-	-	-	-	-	-	1533562	304540.9	198.58
31-32	-	-	40409	140523	202256	303957	116275	148850	7610	55313	18393	15785	-	-	-	-	-	-	1044371	226553.2	216.93
32-33	-	-	-	44168	64097	225825	92930	50064	28724	19502	-	4828	14485	-	-	-	-	-	544623	129560.2	237.89
33-34	-	-	-	48406	26566	257034	64379	84912	-	42729	28354	-	5462	7280	-	-	-	-	565122	149174.5	263.97
34-35	-	-	-	3397	2265	178940	135498	317893	39745	6848	10195	112420	53887	-	-	-	-	-	1013989	291284.0	287.27
35-36	-	-	-	-	-	54636	88250	524634	69648	261730	321495	449952	392923	34834	8385	-	-	-	2206686	667182.3	302.37
36-37	-	-	-	574	-	5793	32651	110594	55438	213444	332450	732314	991171	189498	83353	-	-	-	2767280	875852.2	316.54
37-38	-	-	-	-	-	-	-	10363	31856	48554	108562	386699	546003	225151	76628	9206	-	-	1442722	481643.0	333.84
38-39	-	-	-	-	-	-	-	-	-	2948	12382	46867	208394	81170	24945	17885	9630	-	404221	143821.5	355.80
39-40	-	-	-	-	-	-	-	-	-	-	-	34141	16744	-	7759	-	-	-	58645	21826.6	372.18
40-41	-	-	-	-	-	-	-	-	-	-	-	-	-	-	-	-	-	1005	1005	-	-
TSN(1000)	10739	132104	1062516	4362511	1192292	1521880	874451	1452815	326509	726950	974924	1784745	2229068	537932	201072	27091	9630	14093	17441322	-	-
TSB(1000 kg)	178.0	12195.0	134102.1	740852.4	226865.9	349122.3	205269.0	396325.3	87616.0	215760.4	295730.6	563097.7	716332.0	177948.6	67738.6	9706.0	3719.2	217.8	- 4202777.1	-	-
Mean length (cm)	13.41	22.92	25.40	28.55	29.67	31.69	31.92	33.65	35.35	34.47	35.27	35.95	36.29	36.65	36.82	37.66	38.00	15.38	-	-	-
Mean weight (g)	16.58	92.31	126.21	169.82	190.28	229.40	234.74	272.80	268.34	296.80	303.34	315.51	321.36	330.80	336.89	358.28	386.20	16.64	-	-	240.98

Table A2. IESNS 2017 in the Norwegian Sea. Corrected estimates of abundance, mean weight and mean length of blue whiting.

LenGrp	age 1	2	3	4	5	6	7	8	9	10	11	12	13	14	Number (1E3)	Biomass (1E3kg)	Mean W (g)
17-18	888	-	-	-	-	-	-	-	-	-	-	-	-	-	888	24.9	28.00
18-19	10398	-	-	-	-	-	-	-	-	-	-	-	-	-	10398	363.0	34.91
19-20	149759	-	-	-	-	-	-	-	-	-	-	-	-	-	149759	5968.3	39.85
20-21	477802	10505	1050	2101	-	-	-	-	-	-	-	-	-	-	491458	22488.8	45.76
21-22	441561	120703	17223	-	-	-	-	-	-	-	-	-	-	-	579487	30680.8	52.94
22-23	150338	301374	164217	29957	-	-	-	-	-	-	-	-	-	-	645886	40393.5	62.54
23-24	1416	570459	392353	39080	-	-	-	-	-	-	-	-	-	-	1003308	73677.1	73.43
24-25	-	559031	810208	113490	13412	-	-	-	-	-	-	-	-	-	1496140	124233.8	83.04
25-26	-	365348	1170907	194005	24131	-	-	-	-	-	-	-	-	-	1754392	164146.7	93.56
26-27	-	116902	1027315	307565	24622	-	889	-	-	-	-	-	-	-	1477294	153361.9	103.81
27-28	-	30825	450062	319144	50148	12904	969	-	-	-	-	-	-	-	864051	99827.3	115.53
28-29	4172	11918	119831	169348	77800	23608	8781	-	-	-	-	-	-	-	415459	54422.9	130.99
29-30	-	-	29875	73561	50703	36938	9994	-	-	1110	-	-	-	-	202181	29735.8	147.07
30-31	-	-	16984	10735	36996	42736	40811	-	-	-	-	-	-	-	148262	23816.4	160.64
31-32	-	-	2783	-	85013	15291	6254	1251	-	-	-	-	-	-	110593	19528.3	176.58
32-33	-	-	-	2772	7718	18121	8316	11352	-	5544	9805	-	-	5544	69172	14629.9	211.50
33-34	-	-	-	2350	10246	17297	12596	9402	-	11752	4701	4701	2350	2350	77746	16124.1	207.39
34-35	-	-	-	1891	5622	5622	5622	7713	2811	8433	2811	14825	-	2811	58163	14214.3	244.39
35-36	-	-	-	-	-	-	19464	13917	9278	18557	4639	-	-	-	65856	17901.5	271.83
36-37	-	-	-	-	2897	-	2897	2897	5793	5793	5793	-	-	-	26070	8003.5	307.00
37-38	-	-	-	-	-	-	-	-	4549	4549	-	-	-	-	9098	2563.4	281.75
38-39	-	-	-	-	-	-	-	-	-	-	-	2187	14825	-	17012	5163.2	303.50
39-40	-	-	-	-	-	-	3645	-	-	-	-	-	14825	-	18470	6003.4	325.03
40-41	-	-	-	-	-	-	-	-	-	-	-	1094	-	-	1094	371.8	340.00
TSN(1000)	1236334	2087065	4202809	1266000	389308	172518	120238	46531	22432	55739	27750	22807	32000	10706	9692236	-	-
TSB(1000 kg)	60658.2	163393.9	398269.8	139271.3	56926.9	29458.0	22886.0	11258.6	5967.1	14316.2	7039.6	5945.3	9774.4	2479.1	-	927644.5	-
Mean length (cm)	20.54	23.68	25.21	26.43	28.95	30.22	31.82	33.89	35.77	34.47	33.81	34.51	38.13	32.87	-	-	-
Mean weight (g)	49.06	78.29	94.76	110.01	146.23	170.75	190.34	241.96	266.01	256.84	253.68	260.68	305.45	231.57	-	-	95.71

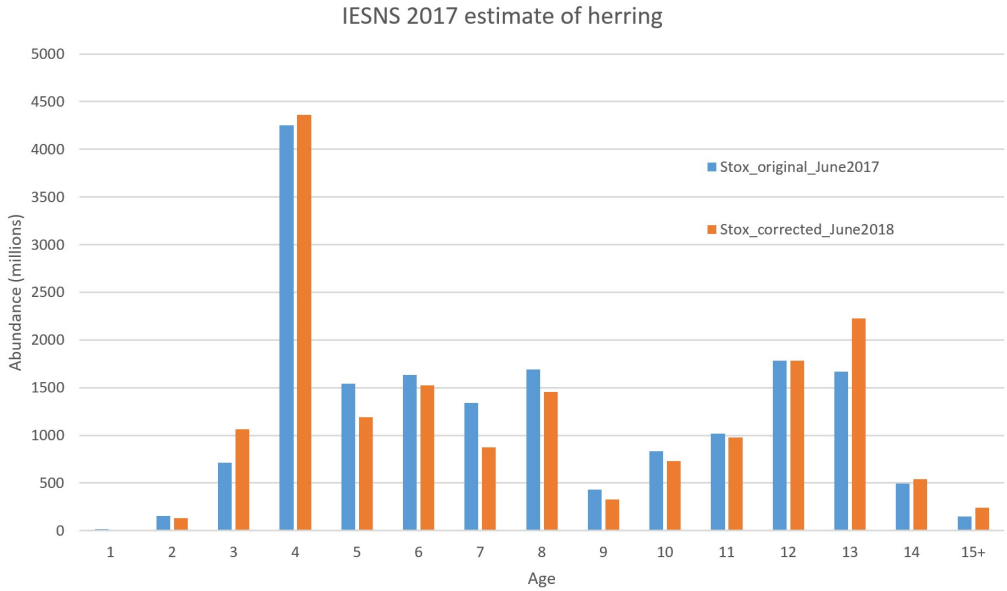

Figure A1. IESNS 2017 in the Norwegian Sea. Original and corrected abundance estimates of Norwegian spring-spawning herring.

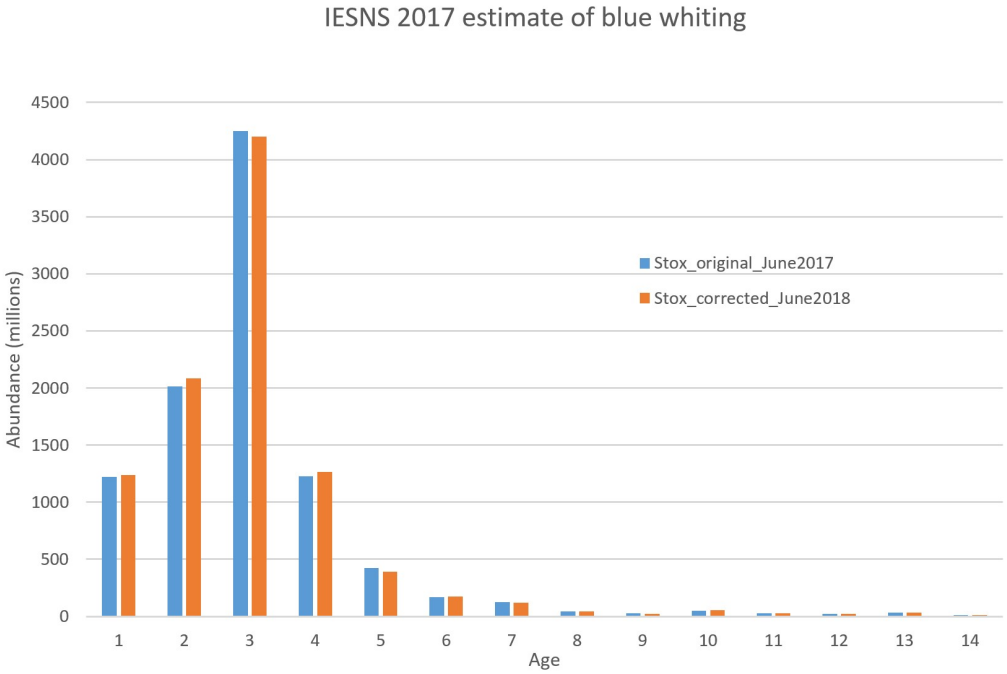

Figure A2. IESNS 2017 in the Norwegian Sea. Original and corrected abundance estimates of blue whiting.

Appendix 2

Observations of Norwegian spring spawning herring (NSSH) using fisheries sonar during international ecosystem survey in Nordic SEA (IESNS) in May – June 2018

Authors: Sindre Vatnehol and Héctor Peña

Contents

1. Introduction:

In acoustic trawl surveys on pelagic schooling species, the down-looking narrow-beam echo sounder is the standard tool used for estimating fish abundance. Bias in the estimate may occur when fish are distributed in the acoustic blind zone of the echo sounder, i.e. between the sea surface and the acoustic far-field distance of the transducer. When transducers are mounted on a drop keel below the vessels hull, this blind zone can extend up to 15 m below the sea surface. Another source of bias may occur when fish avoids the surveying vessel, either due to an horizontal movement or an vertical movement, i.e. diving (De Robertis and Handegard, 2013).

The fisheries sonar is multibeam acoustic systems using horizontal beams in a 360 deg fan around the vessel alternated with vertical beams in a 180 deg fan. The horizontal beams can be electronically steered, being able to measure the fish aggregations in the upper layers up to the sea surface, at long distances (i.e. kilometers) from the vessel. Similarly, the vertical beams can be steered to form a vertical fan that is perpendicular to the vessel track, sampling the entire water column, at both sides of the vessel. These technical

characteristics, together with the high availability of these instruments in most research and commercial fishing vessels, makes sonars into a tool capable of investigating the blind zone and avoidance bias of the echo sounder sampling. Disadvantages of this type of sonar when compared with scientific sonars are a wider beam width (i.e. 5 deg in Simrad SU90) in comparison with scientific sonars (i.e. 4 deg in Simrad MS70), and a reduced dynamic range.

Efforts from the Norwegian Institute of Marine Research, over the last 10 years, includes calibration procedure (Macaulay et al., 2016; Ona et al., 2009) and post-processing system for sonar data, to be used for either single school investigations or for systematic surveys for abundance estimation. Interpretation of sonar data is not part of the routine activity during the IESNS survey, and one objective for this cruise was to do establish a daily routine for interpretation sonar data the first 21 days of the survey. In this report, we present the progress for using sonar as a tool to identify and quantify the bias of the echo sounder estimates.

2. Preparation

2.1 Calibration

The sonar was calibrated in Sandviksflaket on 30th of April, 2018. Weather conditions were good, with low wind speed and low sea height. The procedure for calibration of the fisheries sonar was conducted according to Macaulay et al. (2016), where totally 9 beams were calibrated (3 port, 3 bow and 3 starboard side). 64 mm tungsten carbide was used as a calibration target. The following configuration was used; signal frequency of 26 kHz, FM normal transmission mode, narrow vertical beam and tilt angle of 7 deg. below horizontal. The calibration procedure took 3 hours, including rig mounting, calibrating and demount of the rig. The processing of the calibration data was not made when the results in the present report were made; hence, any values presented in this report are uncalibrated ones.

2.2 Operational settings and procedures

The sonar has two beam configuration modes, the horizontal and the vertical, where alternates between the two configurations for each successive ping. The horizontal mode was configured to sample the echo sounder blind zone, i.e. from surface up to 10-12 m; thus, a beam tilt angle of 5 degrees below horizontal was used. For the vertical mode, a 180° vertical beam fan was set perpendicular to the vessel. The detection range of the sonar was set to 600 m for both beam configurations. The sonar was synchronized in time with the EK80 echo sounder and MS70 scientific sonar to avoid acoustic interference in either equipment. The resulting ping rate of the sonar was between 4 to 5 seconds between measurement of either beam configuration mode. For practical usage, this is too slow ping rate. All the sonar filters (AGC, RCG, Ping to ping) were set to default values, except for the “Noise filter” which was disabled as this corrupts the data. Data in the ‘.raw’ format was collected continuously during the survey and stored in an external 2 TB hard drive and into tape backup system. The ‘.raw’ data was converted to the ICES recommended ‘.nc’ (NetCDF) format.

2.3 Common output file

A similar file to the echo sounder's output file List User File 20 (coined EK80-LUF20) was made for the sonar output. The sonar output files are henceforth coined sonar-LUF20. Using a common output file structure enables direct comparison between the echo sounder and the sonar; and, the sonar output file can be uploaded and used on several processing software, such as Stox. Since the fisheries sonar has two beams' configurations, two sonar-LUF20 files were made for each configuration. The procedure for making the sonar-LUF20 are further described.

2.4 Post-processing of vertical sonar beams (Automatic)

An automatic algorithm was made in PYTHON language to automatically process the sonar data, and convert the data to NASC values,

$$s_A = 4\pi\,(1852)^2\, s_a$$

Here, s_a is the area backscatter coefficient. For the sonar data, a similar approach as shown in Patel and Ona (2009) was used, where only data within a specified range interval (horizontal distance from the vessel) between w_1 and w_2 are used, see figure 2. Consequently,

$$s_a = \int_{w_1}^{w_2}\int_{z_1}^{z_2} s_v\, dz\, dw.$$

At this point, all the s_v values are integrated, even those with background noise and other biological targets. Additional filters are needed to increase the signal-to-noise ratio.

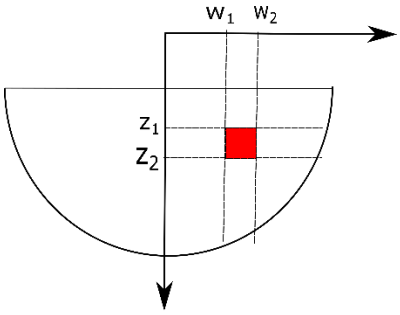

Figure 1Illustration of the echo integration of the vertical beams. All data between the depth interval z_1 and z_2 as well as the distance interval w_1 and w_2 are integrated. One integration bin is identified as the red square.

Background noise filter

The background noise within a time interval can be removed via

$$s_v = \begin{cases} s_v & if \quad s_v \geq \dfrac{\kappa}{t_2 - t_1}\displaystyle\int_{t_1}^{t_2} s_v(r,m,t)\,dt \\ 0 & else \end{cases}$$

where κ is a threshold coefficient. This filter was included for each log distance.

Threshold filter

Targets with low s_v values, hence fish without swim bladder, can be removed via

$$s_v = \begin{cases} s_v & if \;\; s_v \geq s_v^{min} \\ 0 & else \end{cases}$$

Here, s_v^{min} is the minimal s_v value for acceptance where $10 \log_{10} s_v^{min} = -65 \; dB$.

2.5 Post-processing of horizontal sonar beams (PROFOS)

The Processing system for omni directional fisheries sonar (PROFOS) module of the LSSS (Large Scale Survey System, Korneliussen et al., 2016) software was used to process the data. The software has an automatic school detection functionality that was used, and, sequentially, manual quality control and correction of the segmented schools was done. The criteria for school detection was continuously adapted by the user to enable fish schools of different size and shape to be detected. In general, the most common settings were: 10 dB above the background level, minimum surface of 100 m^2, maximum surface of 7000 m^2, two missing pings, at least 10 pings schools, and a ratio of 10 between length and school width.

The output from the PROFOS are s_v values for each data pixel on each school. These values were integrated into 10m x 1nmi bins and converted into NASC values, a similar approach as done for the vertical beams. The conversion from the PROFOS output files to sonar-LUF20 was done using a dedicated R-script.

3. Preliminary result

3.1 Making the common data output

The sonar data collected in vertical mode was integrated into 10 meters depth bins for each 1 nmi distance (vertical, Figure 3 lower panel), In the horizontal mode, acoustic backscattering data from schools detected in the horizontal beams was integrated in one channel where the size was defined by the volume sampled by the sonar (i.e. 10 and 80 m depth). To simplify the comparison, start and stop of each distant channel was identical to that of the EK80-LUF20. Fisheries sonar emits sound with only one signal frequency; hence, a species discrimination using multi-frequency analysis (Fässler et al., 2007; Korneliussen et al., 2016) is not possible. Therefore, the sonar-LUF20 for the vertical beams includes all species, i.e NSSH, mesopelagic fish and blue whiting; however, fish aggregated into schools was labeled as herring for the horizontal beam data. Visual interpretation of the sonar-LUF20 report, Figure 3, identifies the first two depth channels, i.e. 0-20 m, as noisy, largely influenced by near-surface bobbles and waves. Also, specifically for the vertical beams, the seabed was included in the integration. A future development of a bottom filter is needed; however, in the comparison with the echo sounder, this proportion of the data was ignored.

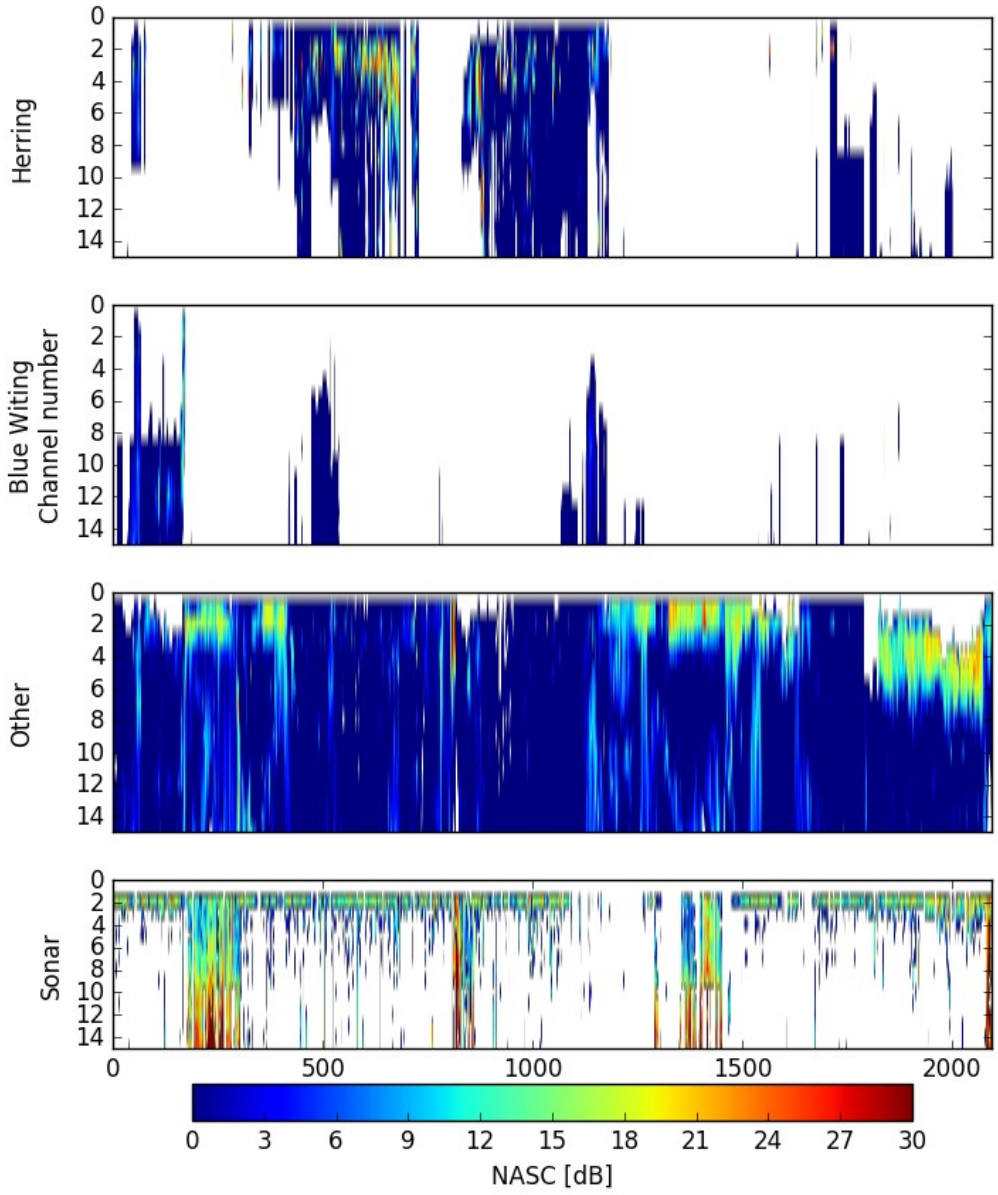

Figure 2. Visualization of EK80-LUF20 file for herring (first upper panel), blue whiting (second upper panel) and other species (third upper panel) and of the sonar-LUF20 (lower panel) using data from Simrad SU90 collected in the vertical mode. The size of the depth channels is 10 m, and the size of the distance channels is 1 nmi. In the lower panel, the data with a NASC value larger than 21 dB is from the seabed, and must be removed in a future development. Higher noise levels are seen in depth channel 1 and 2 in the sonar-LUF20, where this noise origins from air-bobbles and surface waves.

3.2 Comparison with echosounder output

In a preliminary comparison with the echosounder, the NASC information of all species in the EK80-LUF20 were used (Figure 3, three top panel) as the sonar-LUF20 for the vertical beams does not divide the NASC values between species. The vertical distribution, figure 4,

show the sonar record more acoustic energy at 20 m depth than what was recorded of herring by the echosounder; but, the sonar integrates all acoustic energy, also the ones originated from blue whiting, plankton and mesopelagic fish. Also, because the unsuccessful calibration, the values from the sonar must be treated as relative. In the next step for using sonar on routine surveys is to develop statistical models that combines the LUF20 files from several sources, i.e. sonar and echosounder, in order to make a bias-correction LUF20.

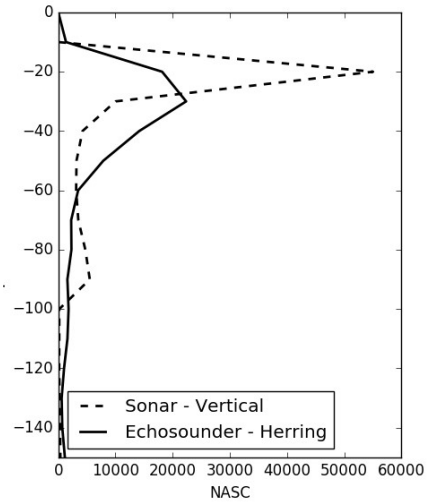

Figure 4. Vertical distribution of herring as recorded by the echosounder (whole line), and the vertical distribution of all scatterers as recorded by the sonar (dotted line)

The analysis of interpreted schools detected within the sonar's horizontal beams, and the acoustics scatters assigned to herring with the echo sounder, are show in Figure 5. Here, it is possible to identify two periods (4.05 to 6.05 and first hours of 10.05) where no herring was allocated in the echo sounder data, and school were detected by the sonar in the same depth layer. Further analysis is needed to identify if this is caused by one of the bias sources, i.e. avoidance or fish in blind zone; and, if so, if these represent a significant contribution of the stock. Analysis of the remaining data from the survey will be analyzed in a later stage.

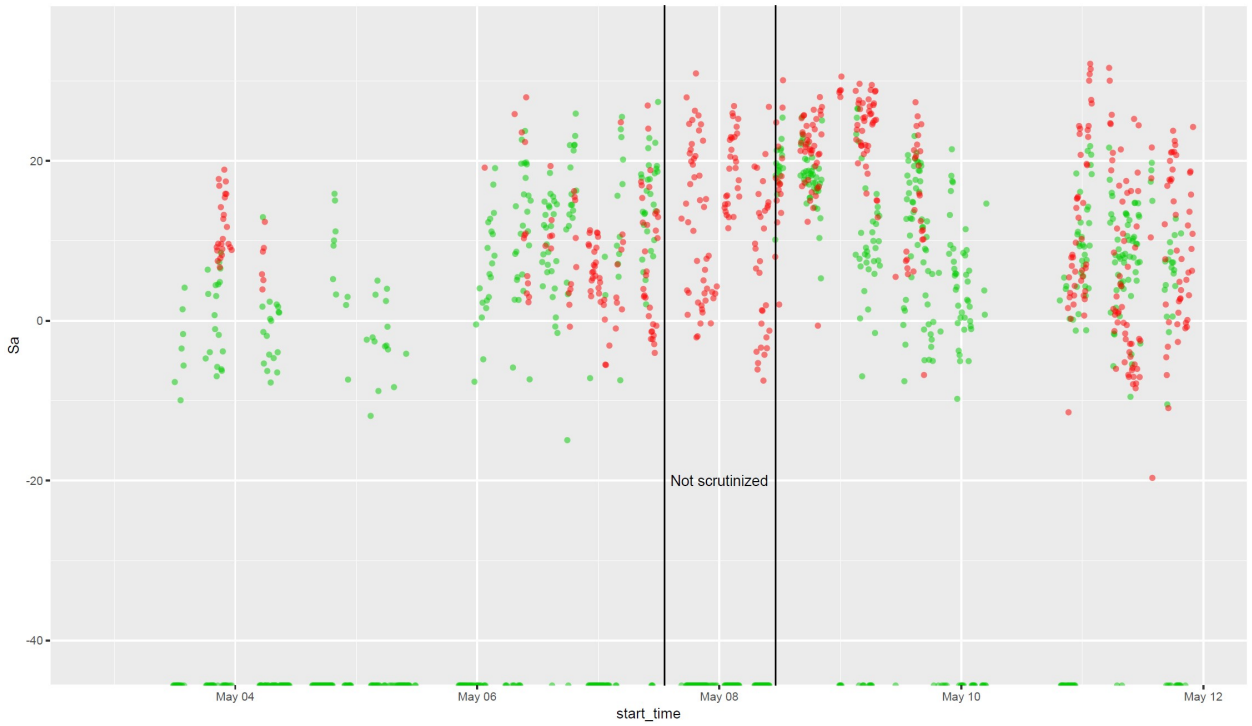

Figure 5. Distribution of schools observed with the sonar (green dots) and herring allocated in the echo sounder (red dots) between 3rd to 12th May. Sa values from sonar and echo sounder are scaled so can be displayed in same level. During a period on May 8th sonar data was not interpreted and indicated in the figure.

3.3 Other sonar results

Implementation

An implicit objective during the survey, was to interpret the horizontal beams the sonar in a daily basis. The interpretation of 24 hours took 4 hours; however, more time was needed when several fish schools were present in the data. The automatic school detection feature in PROFOS performed very good when sea state was calm, and wind speed below 20 knots. When wind increases, noise level increased at ranges around the vessel. A criterion was established to define the sonar exclusion zone around the vessel, and the size of the exclusion zone was optimised to exclude the noisy data (Figure 6). E.g. with noise levels about 20-30 knots the exclusion zone was set up to 300 m; but, with even higher wind speed, the interpretation of the sonar data was not possible, and this proportion of the data was ignored.

Another challenge was to identify when clouds of air-bubbles were interpreted by the automatic detection algorithm as small schools. These features fulfil all the criteria (strength, size, persistence, etc.) used for school detection. The approach to avoid these data to be included was to continuous observe the sonar screen. Candidates that had a strong and well-defined echo in the vertical fan was labelled as herring, while the other was ignored.

In summary, the scrutinizing of the SU90 data during a systematic acoustic survey is doable activity, that requires a dedicated monitoring of the sonar display, frequently record the events in a separate log-book or screen-dumps.

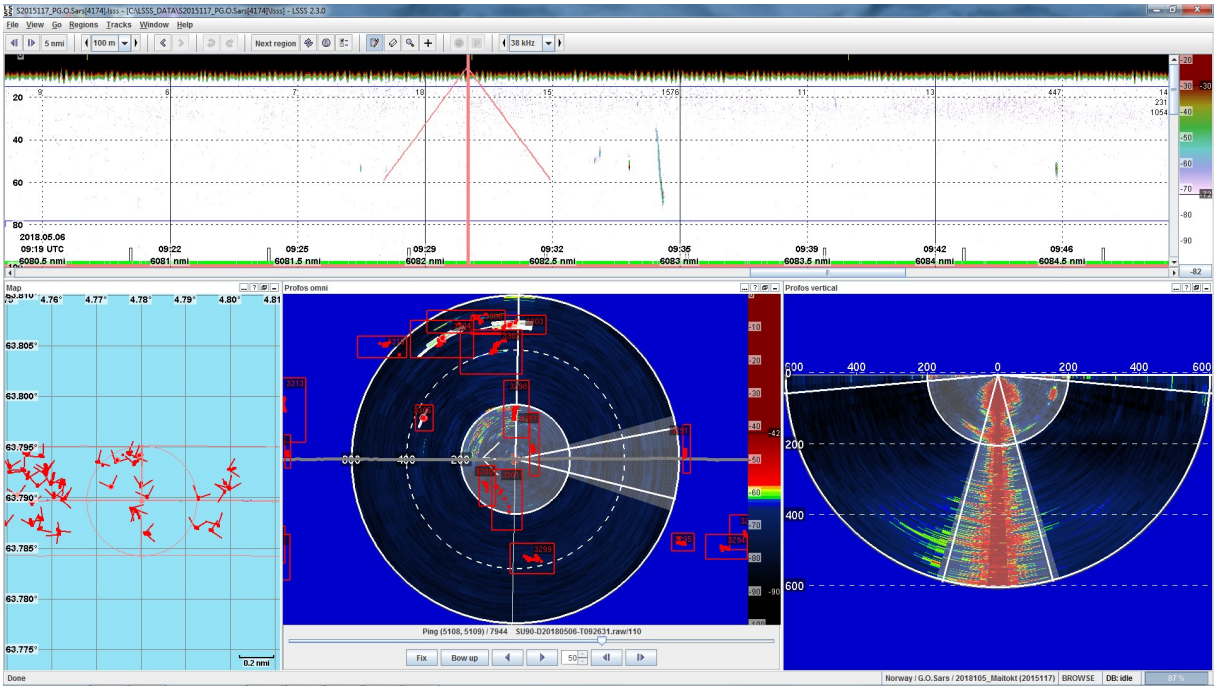

Figure 6. Screen shot of LSSS program showing the EK80 data (upper panel), map with school's detections in the sonar along the track (left bottom), sonar horizontal beams with red dots representing each school detection (centre bottom) and vertical sonar beams (right bottom panel).

Single school biomass estimates from echosounder

The biomass of three schools observed with both the sonar and the echo sounder were made, Table 1, using school parameters derived from the echo sounder measurements. The computed school biomass confirm that the targets observed in the sonar horizontal beams correspond to herring schools, and provides an idea of individual school biomass, which ranges between hundreds of kilos to few tonnes.

	School 1	School 2	School 3

Fish length (cm)	31	35	29
Fish weight (g)	212	340	171
s_A (m^2 nmi^{-2})	7870	69	41697
s_L (m)	115	1	656
Length (nmi)	0.01	0.01	0.02
Length (m)	27.1	26.8	29.1
Mean SV (dB)	-46.0	-64.2	-40.8
Mean TS (dB)	-42.1	-41.0	-42.7
SV-TS (dB)	-3.9	-23.2	1.9
RHO (fish m^{-3})	0.40	0.005	1.53
Radius (m)	13.5	13.4	15
Height (m)	6.0	4.3	10.0
Section area (m^2)	575	566	666
Volume (m^3)	3449	2432	6664
Fish number	1396	12	10208
School biomass (ton)	0.30	3.97E-03	1.75

Table 1. School parameters obtained from EK80 echo sounder measurements. The same schools were previously sampled with the horizontal beams of the fisheries sonar. Fish length and weight were obtained from pelagic trawling. Target strength was computed using equation 20 Log (fish length) -71.9.

Fish school distribution

A general overview of the sonar data shows the presence of rather small fish aggregations in most of the survey track, with more schools observed from the centre of the Norwegian sea to the west (Figure 7). The absence of fish in a few regions correspond to periods of adverse weather conditions (wind speed above 25 knots), in which it was not possible to interpret the data because of the increased noise level.

Based in the school and vessel geographical position, the distance of each school to the vessel track on each ping was computed (Figure 8, left panel). Most of the school detections occurred 100 m from the vessel track, with a decrease of schools' detection at closer distances, a consequence of a reduced sampling volume. The centre depth of the schools detected by the sonar had a normal distribution with a maximum of schools at about 30 m depth (Figure 8, right panel). The minimum central school depth was 11 m, and a maximum of 62 m. The depth distribution of the schools depends on the tilt angle of the horizontal fan and the vertical beam opening and the operational sonar range. Therefore, there is a detection probability of the schools at different depth, i.e. at shallower depths the sampling surface of the horizontal fan is reduced in comparison with mid and large ranges. It is required to estimate the theoretical detection to obtain a realistic vertical school distribution.

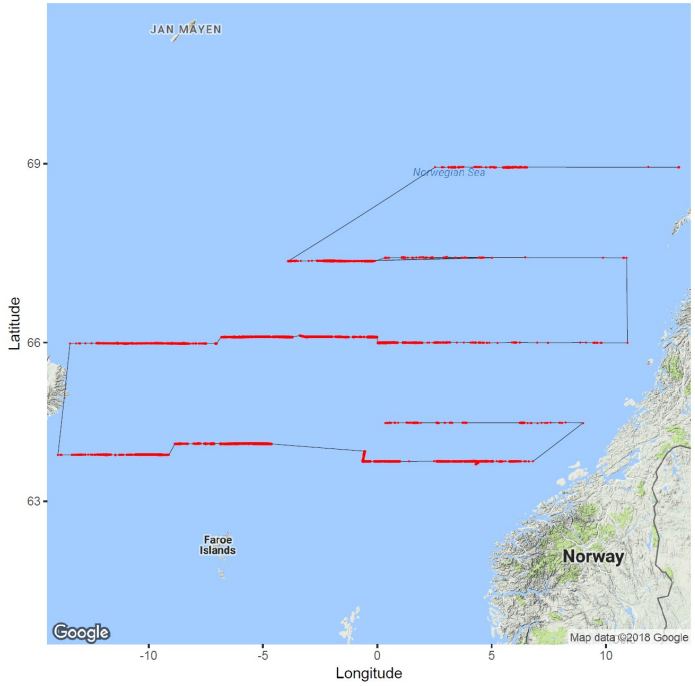

Figure 7. Map showing the survey track from R/V G.O. Sars between 30 April to 21 June. Red dots represent fish aggregations detected within SU90 fisheries sonar's horizontal beams.

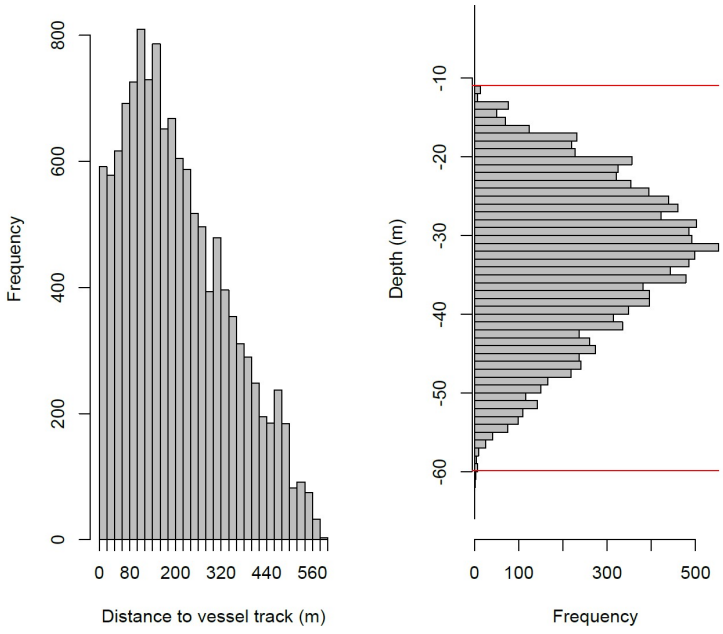

Figure 8. School distance to the vessel track (left panel) and centre depth of schools (right panel).

Fish migration

The mean swimming speed of the schools aggregated by 1 nmi was below 1 knot (Figure 8, left panel). There is not a clear predominant swimming direction. In the northerly transect more schools are swimming north and in transect centred in 66° N a general west direction is observed. When accumulate the migration data of all schools, the polar histogram confirms the absence of a general migration direction during the survey period (Figure 9, right panel).

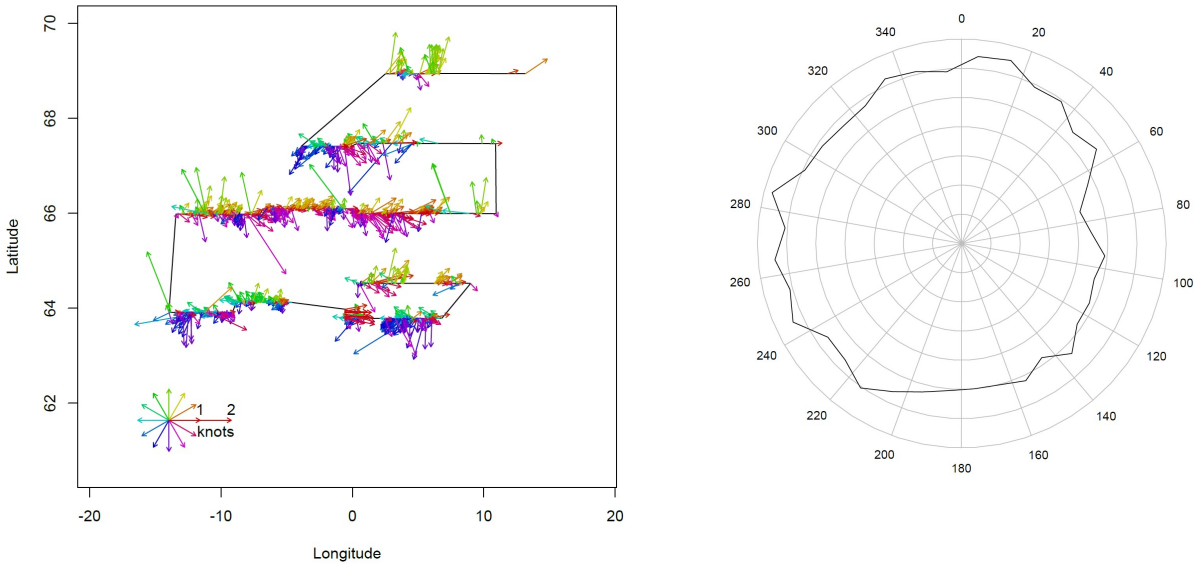

Figure 9. Mean school speed and direction aggregated by 1 nmi along the cruise track (left panel) and polar histogram of school direction (right panel).

4. References:

5. Fässler, S. M. M., Santos, R., García-Núñez, N., and Fernandes, P. G. (2007). "Multifrequency backscattering properties of Atlantic herring (Clupea harengus) and Norway pout (Trisopterus esmarkii)," Can. J. Fish. Aquat. Sci., 64, 362–374. doi:10.1139/f07-013

6. Korneliussen, R. J., Heggelund, Y., Macaulay, G. J., Patel, D., Johnsen, E., and Eliassen, I. K. (2016). "Acoustic identification of marine species using a feature library," Methods Oceanogr., 17, 187–205. doi:10.1016/j.mio.2016.09.002

7. Macaulay, G. J., Vatnehol, S., Gammelsæter, O. B., Ona, E., and Pena, H. (2016). "Practical calibration of ship-mounted omni-directional fisheries sonars," Methods Oceanogr., 17, 206--220.

8. Ona, E., Mazauric, V., and Andersen, L. N. (2009). "Calibration methods for two scientific multibeam systems," ICES J. Mar. Sci., 66, 1326–1334. doi:10.1093/icesjms/fsp125

9. Patel, R., and Ona, E. (2009). "Measuring herring densities with one real and several phantom research vessels," ICES J. Mar. Sci. J. du Cons., 66, 1264–1269. doi:10.1093/icesjms/fsp128

10. De Robertis, A., and Handegard, N. O. (2013). "Fish avoidance of research vessels and the efficacy of noise-reduced vessels: A review," ICES J. Mar. Sci., 70, 34–45. doi:10.1093/icesjms/fss155

Appendix 3

Observations of Norwegian spring spawning herring (NSSH) using scientific and fisheries sonar during international ecosystem survey in Nordic SEA (IESNS) in May – June 2018

Author:Rolf Korneliussen

4. Scientific sonar – Simrad MS70

4.1 Calibration

The sonar MS70 was calibrated in Sandviksflaket on 30th of April 2018. Weather conditions were good, with low wind speed and low sea height. The calibration of the scientific sonar was conducted according to procedures described in Ona et a. (2009). The 500 port oriented beams of MS70 covers 60˚ horizontally x 45 ˚ vertically from a transducer with center at 7.5 m depth when operated. MS70 transmits 20 vertical fans, with the highest frequency (112 kHz) aiming 45˚ downwards relative to the surface and the lowest frequency (75 kHz) aiming horizontally, i.e. at 0˚. Due to the span of the frequencies, there was a need to use two calibration spheres: a 75-mm diameter and 84-mm tungsten-carbide with 6% cobalt binder.

4.2 Data collection

The sonar was operated in continuous-wave mode, with pulse duration of 2 ms and a data collection range of 350 m. Four fan beams transmitted simultaneously (i.e. 112 kHz at 45 ˚, 113.9 kHz at 47.5 ˚, 115.7 kHz at 50 ˚, and 117.6 kHz at 52.5 ˚ transmitted concurrently, followed by the next four, etc.). Therefore, all pulses with 2 ms duration were transmitted during 10 ms. The beam widths were between 3˚ and 4 ˚ varying vertically with the frequency. The first side lobe was -35 dB relative to the main lobe vertically, and -25 dB horizontally. Using data from the MRU, the sonar automatically compensated for roll of up to 10˚. The sonar pings were synchronized with those of the echosounder, typically at a frequency of 1.2 Hz. The relatively short range of MS70 was used to be able to maintain the same ping-rate as for the echo sounder EK80.

The MS70 sonar had increasingly technical problems during the survey, with increasing number of bad samples in the pings. From May 15 MS70 was only sporadically functioning, and at the beginning of May 17 it was turned off for good.

4.3 Preprocessing

The sonar was operated in continuous-wave mode, with pulse duration of 2 ms and a data collection range of 350 m. Four fan beams transmitted simultaneously (i.e. 112 kHz at 45 ˚, 113.9 kHz at 47.5 ˚, 115.7 kHz at 50 ˚, and 117.6 kHz at 52.5 ˚ transmitted concurrently, followed by the next four, etc.). Therefore, all pulses with 2 ms duration were transmitted during 10 ms. The beam widths were between 3˚ and 4 ˚ varying vertically with the frequency. The first side lobe was -35 dB relative to the main lobe vertically, and -25 dB horizontally. Using data from the MRU, the sonar automatically compensated for roll of up to 10˚. The sonar pings were synchronized with those of the echosounder, typically at a

frequency of 1.2 Hz. The relatively short range of MS70 was used to be able to maintain the same ping-rate as for the echo sounder EK80.

The MS70 data were processed with the PROMUS (Processing system for advanced multibeam sonar) module (Korneliussen et al., 2009) of LSSS (Korneliussen et al., 2016). The data were pre-processed with KORONA by means of processing modules dedicated for MS70 data. Pre-processing means that the processing was done automatically without interference from the operator. The modules were used to: (1) Remove of spatial and temporal spikes; (2) Reduce data; (3) Detect schools automatically; (4) Detect bad data; The results from the pre-processing were made available to the operator for use during scrutiny, and the operator than decided which parts of the information should be used. Some modules were run sequentially with different settings, to perform different tasks. The detailed KORONA-PROMUS setup may not be of interest, but they are listed below for reference. The setup for pre-processing MS70 data were:

1) *Reduce data:*
   - *remove all data with a horizontal distance to the ship less than 30 m.*
   - *Remove outer parts of beam at ranges where the upper edge hits surface*
2) *Spike-filter: remove wall-shaped spatial spikes > -45 dB and 15 dB stronger than surroundings*
3) *Spike-filter: remove pencil-beam-shaped spatial spikes > -45 dB and 15 dB stronger than surroundings*
4) *Spike-filter: remove temporal spikes > -45 dB and 15 dB stronger than surroundings*
5) *Smooth along beam with an 8 m Gaussian kernel*
6) *Quantify ambient noise: use the 175 outermost meters of each beam to estimate noise. The slowly varying ambient noise is used further, i.e. a noise-estimate for the ambient noise of each beam based on data from the whole survey.*
7) *Reduce data (Not done previously to make spike-removal and estimation of ambient noise better)*
   - *Remove all data at more than 250 horizontal distance from the ship*
   - *Remove the outmost part of beams where uppermost edge is closer to surface than 4 m*
8) *Correct data for ambient noise*
9) *Spike-filter: remove spikes > -70 dB (of corrected data) shaped as vertical fans and 20 dB stronger than surroundings*
10) *Spike-filter: remove spikes > -70 dB (of corrected data) shaped as pencil-beams and 20 dB stronger than surroundings*
11) *Remove all samples stronger than -25 dB and weaker than -70 dB*
12) *Detect schools using K-means clustering*
13) *Compress data*
14) *Detect bad pings*

4.4 MS70 data interpretation

The preprocessing removed most spike-noise and corrected for ambient noise. During the manual scrutiny, some pings were manually marked for exclusion and not used further. The scrutiny of the echosounder data is done by a team consisting of ***at least*** the instrument chief and the cruise leader. The result of the discussion during the scrutiny is essential for the quality of the scrutinized data. Ideally, the MS70 data should have been scrutinized together with EK80 data. As the expected processing-speed of the MS70 data were expected to be too slow for co-scrutinize simultaneous with the EK80 data, those data were intended to be scrutinized during the survey closely after the scrutiny of the echosounder. Unlike the EK80 data scrutinized by a team of two, the MS70 data were scrutinized by one scientist only. The processing was not much faster than real-time during the first days of the survey, which made it challenging to keep up with survey activities in the same manner as during the 2017 survey. The MS70 processing eventually became slower than real-time, which made it impossible to keep up with the survey activities. Most of the time after the survey has been used to improve speed of the both the pre-processing, the semi-automatic processing, and to automate some of the manual work. The speed is currently 60 times faster than during the survey. Analysis of 24 hours of MS70 data typically took 45 – 60

minutes in front of the screen on a laptop after the survey, with the potential of reducing that to 25 minutes (on a laptop).

2D data based on the 4D MS70 data were used to extract 2D-phantom echograms. These echograms were used to get an overview and identify locations of schools in addition to the automatic detection from step 12 above. After the improvement of speed and functionality, the following procedure was used: (1) Data were pre-processed as described above. (2) Chunks of typically 12 hours were loaded into the PC. Bad pings were automatically detected during pre-processing, and were marked as excluded during scrutiny. Schools candidates were automatically detected and grown in 4 dimensions (3 spatial + time). A set of requirements were used to start growing: In most cases, the samples were required to be above 150 m stronger than -58 dB, and weaker than -35 dB. Depending on weather, the schools were in most cases required to not be shallower than 10 – 18 m, but on some occasions, they could be as shallow as 4 m or as deep as 35 m. When grown, a set of criteria were used for automatically rejecting the school-candidate. These were: (A) Minimum (uncorrected) volume 225 m^3; (B) Minimum (uncorrected) height: 90 m; (C) Maximum aspect ratio (uncorrected data): 4; (D) Minimum number of pings: 2; Minimum s_V x Volume: 500; (E) Maximum s_V x Volume: 5 x 10^8. Note that $s_V \equiv 4\pi 1852^2 s_v$. This detection of school candidates typically took 5 minutes for 12 hours of data. The school-candidates were sorted on Volume, upper depth of school and average s_V in addition to the variables listed above, and inspected and potentially removed. There were on average 3500 school candidates in 12 hours of data, of which typically 5-10% were rejected. This process of removing bad school-candidates typically took 15 minutes for 12 hours of data.

The scrutiny itself were usually quite fast as there were mostly two candidate species: herring and blue whiting. Blue whiting was commonly deeper than herring, and for MS70 no schools were considered below 150 m, that is 150 m for the MS70 beam centers: the lower edge of beam could be deeper. The scrutiny for the data May 9-10 were challenging as much backscatter close to the surface due to bubbles and mesopelagic fish. Figure 4.1 shows a screen-grab of LSSS-PROMUS, and the 2m x 2m x 2m grid for representing two different schools close to the surface.

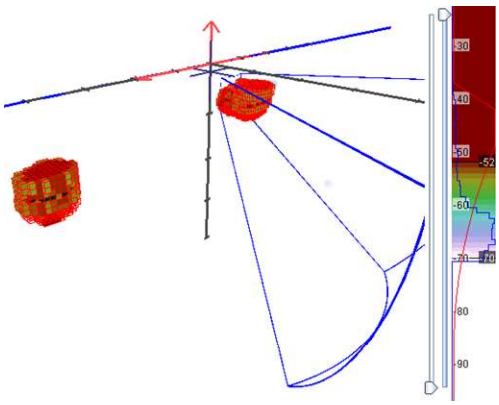

Figure 4.1. LSSS-PROMUS and grid representing two grown schools.

4.5 Results

The results of the data scrutiny were grouped into 5 segments based on its location in two stratas along the cruise-line. Data from (1) May 3, 11:30 – May 5, 02:30 (UTC); (2) May 5

20:15 – May 7, 12:00 (UTC); (5) May 13, 00:00 – May 14, 17:00 (UTC) were in the eastern strata closest to Norway. Data from (3) May 7, 12:00 – May 10, 05:15 (UTC); (4) May 10 19:30 – May 12, 24:00 (UTC); **Figure 4.1** below shows the vertical distribution of herring backscatter for those 5 different regions.

Figure 4.3 shows the vertical distribution of backscatter of the vertical oriented echo sounder EK80 and the sonar MS70 covering horizontal to 45 degrees down of all scrutinized data from May 3, 11:40 – May 14, 17:00 (UTC). The EK80 and MS70 data are not directly comparable, since EK80 stores data as s_A (NASC, i.e. s_V * depth_range), while the MS70 data are stored as s_V (i.e. density). Furthermore, based on simulations the TS-relation of grazing incidence is 3 – 6 dB lower than dorsal side depending on frequency and grazing angle. Previous research has indicated that avoidance reaction is weak below 80 m depth, and therefore the MS70 and EK80 data are normalized so that they are approximately similar in the depth range below 80 m. The frequency and gracing angle dependency on the TS relation Figure 4.2 makes the comparison at e.g. 40-50 m depth between EK80 and MS70 uncertain. Further, notice that the functionality of PROMUS was updated until this report was made, so there may be some miscalculations.

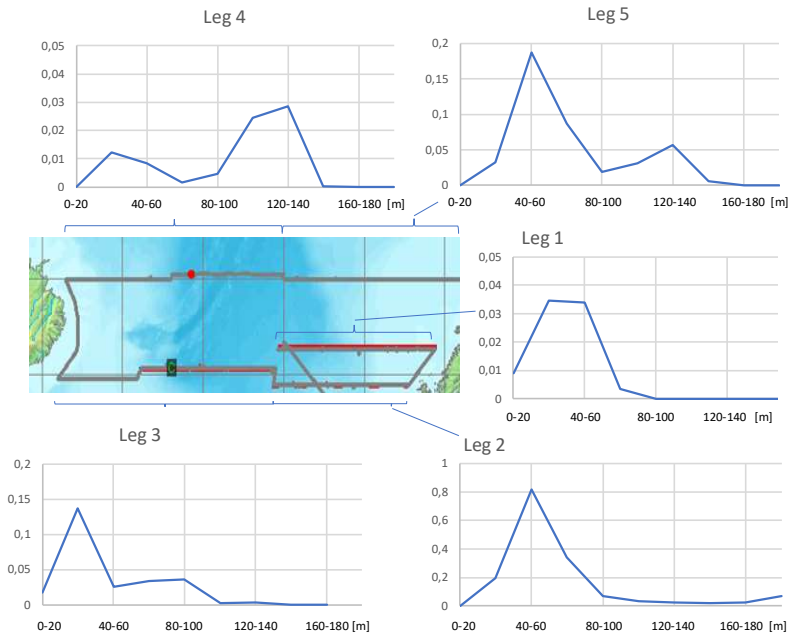

Figure 4.2. Vertical distribution of acoustic backscatter from herring as measured by MS70 onboard FRV "G.O. Sars".

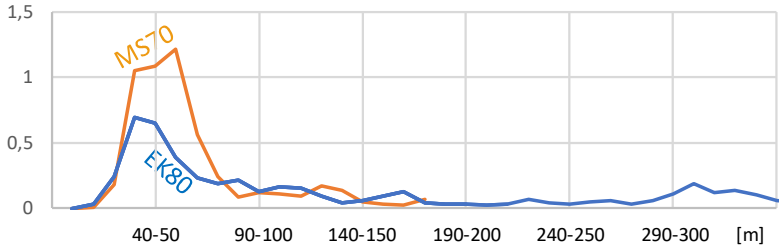

Figure 4.3. Vertical distribution of herring backscatter: EK80, MS70

Although Figures 4.2 and 4.3 are quite simple, they show essentially that there is no need for correcting the acoustic abundance that was measured EK80, at least not in this region.

References:

Korneliussen, R. J., Heggelund, Y., Eliassen, I. K., Øye, O. K., Knutsen, T., and Dalen, J. (**2009**). Combining multibeam-sonar and multifrequencyechosounder data: examples of the analysis and imaging of large euphausiid schools," ICES J. Mar. Sci., **66**: 991–997. doi: 10.1093/icesjms/fsp092

Korneliussen, R. J., Heggelund, Y., Macaulay, G. J., Patel, D., Johnsen, E., and Eliassen. (**2016**). Acoustic identification of marine species using a feature library. Methods in Oceanography, **17**, 187–205. doi: 10.1016/j.mio.2016.09.002

Appendix 4

First trial of Deep Vision

Authors: Sindre Vatnehol and Vaneeda Allken.

The Deep Vision is a box-unit mounted between the trawl and the cod-end (Rosen et al., 2013). The unit includes a depth sensor, a computer, lights and a stereo-camera system; and recorded 5 frames/seconds (on each camera). This system was used on all trawl hauls but the last, on the first leg on G. O. Sars; and consequently, more than 2 million pictures were taken. The system can estimate the size of the species by manually identifying the snout and the tail of each fish; but this feature was not used.

This was the first time this system was implemented on a routine survey using personnel without detailed knowledge of the system. The equipment was experienced as easy to operate, but transferring data between unit and a topside computer was slow. Handling the large quantity of files proved to be an issue, i.e. loading the files into the LSSS frequently failed. Suggestions to optimize the operation and data handling were frequently forwarded to the equipment's manufacturer. Also, the issues regarding the Deep Vision unit were characterized as minor.

The picture files and the depth sensor log were loaded into the LSSS system. The information was used to identify the depth at which the fish were caught and whether there were some species too small to be caught by the trawl. We regard this as valuable information when interpreting the echosounder data. Future development, such as identification of empty pictures, automatic target and species detections algorithms and automatic length estimation are appreciated as part of the routine survey.

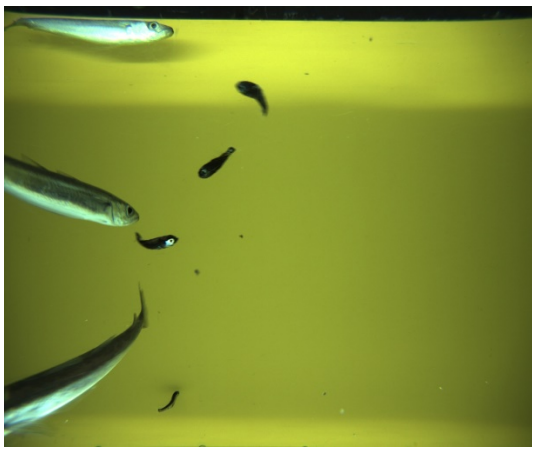

Figure 3 One picture collected from the right-side camera on the Deep-Vision unit.

Rosen, S., Jörgensen, T., Hammersland-White, D., Holst, J. C., and Grant, J. (**2013**). "DeepVision: a stereo camera system provides highly accurate counts and lengths of fish passing inside a trawl," Can. J. Fish. Aquat. Sci., **70**, 1456–1467.